



# HHS Public Access

Author manuscript

ACS Nano. Author manuscript; available in PMC 2022 May 30.

Published in final edited form as:

ACS Nano. 2020 December 22; 14(12): 16220–16240. doi:10.1021/acsnano.0c06336.

## Microfluidic Isolation and Enrichment of Nanoparticles

### Yuliang Xie

Roy J. Carver Department of Biomedical Engineering, University of Iowa, Iowa City, Iowa 52242, United States

### Joseph Rufo,

### Ruoyu Zhong

Department of Mechanical Engineering and Materials Science, Duke University, Durham, North Carolina 27708, United States

### Joseph Rich,

Department of Biomedical Engineering, Duke University, Durham, North Carolina 27708, United States

### Peng Li,

C. Eugene Bennett Department of Chemistry, West Virginia University, Morgantown, West Virginia 26506, United States

### Kam W. Leong,

Department of Biomedical Engineering, Columbia University, New York, New York 10032, United States

### Tony Jun Huang

Department of Mechanical Engineering and Materials Science, Duke University, Durham, North Carolina 27708, United States

## Abstract

Over the past decades, nanoparticles have increased in implementation to a variety of applications ranging from high-efficiency electronics to targeted drug delivery. Recently, microfluidic techniques have become an important tool to isolate and enrich populations of nanoparticles with uniform properties (*e.g.*, size, shape, charge) due to their precision, versatility, and scalability. However, due to the large number of microfluidic techniques available, it can be challenging to identify the most suitable approach for isolating or enriching a nanoparticle of interest. In this review article, we survey microfluidic methods for nanoparticle isolation and enrichment based on their underlying mechanisms, including acoustofluidics, dielectrophoresis,

---

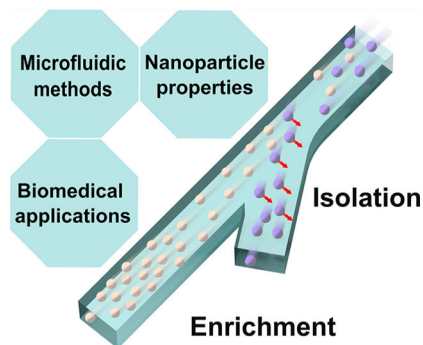
**Corresponding Authors:** **Yuliang Xie** – Roy J. Carver Department of Biomedical Engineering, University of Iowa, Iowa City, Iowa 52242, United States; yuliang-xie@uiowa.edu, **Peng Li** – C. Eugene Bennett Department of Chemistry, West Virginia University, Morgantown, West Virginia 26506, United States; Peng.Li@mail.wvu.edu, **Kam W. Leong** – Department of Biomedical Engineering, Columbia University, New York, New York 10032, United States; kam.leong@columbia.edu, **Tony Jun Huang** – Department of Mechanical Engineering and Materials Science, Duke University, Durham, North Carolina 27708, United States; tony.huang@duke.edu.

Complete contact information is available at: <https://pubs.acs.org/10.1021/acsnano.0c06336>

The authors declare the following competing financial interest(s): T.J.H. has co-founded a start-up company, Ascent Bio-Nano Technologies Inc., to commercialize technologies involving acoustofluidics and acoustic tweezers.

filtration, deterministic lateral displacement, inertial microfluidics, optofluidics, electrophoresis, and affinity-based methods. We discuss the principles, applications, advantages, and limitations of each method. We also provide comparisons with bulk methods, perspectives for future developments and commercialization, and next-generation applications in chemistry, biology, and medicine.

## Graphical Abstract



## Keywords

nanoparticles; isolation; enrichment; microfluidics; acoustofluidics; optofluidics; inertial microfluidics; dielectrophoresis; microfiltration; deterministic lateral displacement

For decades, nanoparticles have drawn significant attention from the scientific communities because their chemical and physical properties differ markedly from those of the bulk material.<sup>1–3</sup> Defined as a particle with characteristic lengths of approximately 100 nm or less, nanoparticles roughly comprise both “soft nanoparticles” (*i.e.*, naturally existing nanoparticles such as proteins, DNAs, viruses, and exosomes) and “hard nanoparticles” (*i.e.*, synthesized inorganic nanoparticles such as gold, silver, and silicon). Today, nanoparticles are widely used in many fields such as catalysis,<sup>4,5</sup> electronics,<sup>6,7</sup> biology,<sup>8,9</sup> and medicine,<sup>10–15</sup> which can be readily witnessed by both the rapidly expanding market size as well as the ever-increasing number of scientific publications.

With the enormous amount of research on nanoparticles, it is broadly recognized that a homogeneous size, shape, charge, and/or chirality of nanoparticles usually greatly enhance their performance in various applications. For example, the optical properties of nanoparticles (*e.g.*, Raman spectra,<sup>16</sup> absorption,<sup>17</sup> and plasmonic features<sup>18</sup>) are highly dependent on their size distribution.<sup>19</sup> As a result, when using nanoparticles in biosensing applications, it is essential to have nanoparticles with a narrow size distribution. The homogeneity in the size of the nanoparticles also impacts their therapeutic efficacy.<sup>20</sup> For example, the capability of nanoparticles to penetrate the blood-brain barrier<sup>21–24</sup> or remain in circulation in the blood<sup>25–29</sup> is largely determined by their size. A homogeneous size distribution also reduces unintended side effects of cytotoxicity.<sup>30–35</sup> In addition to size, homogeneity in the shape and chirality of nanoparticles helps control their interaction with cells,<sup>36</sup> thereby impacting efficacy and bioavailability in therapeutic applications.<sup>37–39</sup> However, most nanoparticle fabrication procedures are prone to impurities, producing

particles with undesired shapes and sizes. As a result, the rigorous development of postfabrication methods to enhance the homogeneity of nanoparticles is essential to advancing nanoparticle research and applications.

Isolation and enrichment are two complementary steps to improve the homogeneity of nanoparticles. Isolation is a process that acts as a selective barrier allowing relatively free passage of one component while retaining or deflecting other components.<sup>40,41</sup> After isolation, the concentration of nanoparticles might decrease due to a loss of particles or the introduction of additional fluids; therefore, an enrichment procedure<sup>42</sup> is often conducted to increase the concentration of specific nanoparticles for collection. Enrichment can also be used to enhance the local concentration of nanoparticles to facilitate detection.<sup>43</sup> It should be noted that some techniques, such as density gradient centrifugation,<sup>44</sup> are capable of simultaneously isolating and enriching nanoparticles.

Microfluidics is one of the emerging techniques that meets the growing and divergent needs for nanoparticle isolation and enrichment.<sup>45,46</sup> Developed in the 1990s, microfluidics has grown as a multidisciplinary field that involves physics, chemistry, engineering, and nanotechnology and has succeeded in isolating and enriching a wide spectrum of nanoparticles. To cover recent advances and offer future perspectives on microfluidic nanoparticle isolation and enrichment, we have written this review article for readers from diverse disciplines and backgrounds. In this article, we will survey current microfluidic methods according to their technical mechanisms (*e.g.*, acoustics, optics, dielectrophoresis, and filtration), and we will discuss both isolation and enrichment, if applicable (Figure 1). We will also provide a summary table of potential solutions for specific particle properties (*e.g.*, size, shape, and charge), with the advantages and limitations of each technique (Table 1). To be more focused and concise, we will confine the scope of “microfluidics” to devices with characteristic lengths of approximately 100  $\mu\text{m}$  or less. As an exclusion, we will not cover methods like high-performance liquid chromatography (HPLC)<sup>47–50</sup> or capillary electrophoresis,<sup>51–55</sup> although they operate at the micrometer scale; readers are referred to excellent reviews on those techniques elsewhere.<sup>47–55</sup>

## ACOUSTOFLUIDICS

Acoustofluidics,<sup>56–66</sup> an approach that integrates acoustic manipulation with microfluidic devices, can efficiently separate nanoparticles. In principle, particles in acoustic fields deflect based on their material properties (*e.g.*, density and compressibility) and size (*i.e.*, volume).<sup>67–72</sup> Researchers discovered that nanoparticles are influenced by the external acoustic field, resulting in trapping, focusing, and patterning,<sup>43,73</sup> enabling nanoparticle separation with acoustofluidic methods. Wu *et al.* demonstrated the separation of a mixture of 500 and 110 nm polystyrene particles, using a 4  $\mu\text{L min}^{-1}$  flow rate for the sample and a 12  $\mu\text{L min}^{-1}$  flow rate for the sheath flow (Figure 2A,B). The yield of 110 nm nanoparticles can reach as high as 90.7%.<sup>74</sup> With a longer distance for particle deflection, researchers achieved separation of polystyrene particles with sizes of 300 and 500 nm.<sup>75</sup> Since acoustofluidic methods operate with powers ( $10^{-2}$ – $10 \text{ W/cm}^2$ ) and frequencies (1 kHz to 500 MHz) in a range similar to those used in ultrasonic imaging (2–18 MHz, less than 1  $\text{W/cm}^2$ ),<sup>57</sup> they often have excellent biocompatibility. Based on the separation performance

of nanometer-sized polystyrene particles, Wu *et al.*<sup>76</sup> further developed an acoustofluidic exosome isolation technique. Their design makes use of two separate, but connected, modules: the first module removes larger, microscale blood components, while the second module is an extracellular vesicle separation unit that removes larger microvesicles and isolates exosomes. Through integration of two components, they were able to isolate exosomes with 98.4% purity from a mixture containing both microvesicles and exosomes, and demonstrated a blood cell removal rate of over 99.999%. Similarly, other types of extracellular vesicles can also be separated with acoustofluidics. Lee *et al.*<sup>77</sup> demonstrated an “acoustic nanofilter” system that size-specifically separates microvesicles in a continuous manner. They applied the acoustic nanofilter to isolate nanoscale (<200 nm) vesicles from cell culture media as well as microvesicles in stored red blood cell products and achieved a >90% separation yield (Figure 2C,D).

Acoustofluidic methods also enrich, concentrate, or trap nanoparticles, which can be integrated after nanoparticle isolation for better recovery or visualization. Nanoparticle enrichment is usually achieved through acoustic radiation force,<sup>72</sup> acoustic streaming,<sup>71</sup> or a combination of both. For instance, Mao *et al.*<sup>43</sup> presented an acoustofluidic chip that can concentrate nanometer-sized particles at the central line of a glass capillary (Figure 3A,B). Nanoparticle enrichment is achieved through the combined effect of the acoustic radiation force with vortex acoustic streaming. They demonstrated the focusing of silica and polystyrene particles with diameters ranging from 80 to 500 nm and the ability to integrate this process with downstream immunoassays. Collins *et al.*<sup>78</sup> introduced highly focused surface acoustic waves at frequencies between 193 and 636 MHz that generate localized acoustic streaming vortices on microfluidic length scales. They can capture nanoparticles as small as 300 nm in diameter and enrich them at a point near the transducer. When the acoustic frequency is increased to the gigahertz regime, Cui *et al.*<sup>79</sup> demonstrated the concentration of 87 nm particles through an acoustic streaming vortex with their hypersonic-induced hydrodynamic tweezers. Other than acoustic streaming, Reyes *et al.*<sup>80</sup> used primary radiation forces in bulk acoustic standing waves for concentrating nanoparticles. They successfully demonstrated the concentration of 200 nm gold nanoparticles at acoustic pressure nodes (Figure 3C–E).

In isolating biological nanoparticles, acoustofluidic methods avoid high shear stresses, high temperatures, or requirements for special liquid media. They allow for label-free isolations based on differences in size or other physical properties. A microfluidic channel provides precise fluid control during acoustic operation. In microfluidic devices, low Reynolds number (*i.e.*, laminar flow) enabled high separation resolution that is not possible in bulk fluid. Acoustofluidic nanoparticle isolation is mainly based on exploiting differences in the size of particles. Furthermore, acoustofluidic devices can potentially be integrated to achieve isolation and enrichment in one system. Current limitations of acoustofluidics mainly arise from instrumentation. Bulky, expensive, and specialized electronics (such as function generators and amplifiers) involved in most acoustofluidic devices limit their widespread use in industrial applications. However, in recent years, much research has gone into developing low-cost,<sup>81–83</sup> open-source<sup>84</sup> alternatives to popularize acoustofluidic devices.

## MICROFLUIDIC DIELECTROPHORESIS

Microfluidic dielectrophoresis (DEP) describes the motion of a dielectric particle in a nonuniform electric field as a result of the polarization effect in a microfluidic device.<sup>85–90</sup> DEP has been extensively studied in isolating and enriching a variety of nanoparticles.<sup>87,91–97</sup> For example, Viefhues *et al.*<sup>98</sup> developed a DEP-based device to separate polystyrene nanoparticles of 20 and 100 nm. They found that 85–100% of the large nanoparticles were deflected and expected that efficient and separation would be possible for nanoparticles that differ by about 30% in diameter. Zhao *et al.*<sup>99</sup> separated nanoparticles with DEP using a nonuniform DC electric field (DC-DEP). In this approach, the electrical conductivity of the suspending solution is adjusted so that the polystyrene nanoparticles of a given size experience positive DEP while the polystyrene nanoparticles of another size experience negative DEP. Using this method, the separation of 51 and 140 nm nanoparticles and the separation of 140 and 500 nm nanoparticles were demonstrated (Figure 4A–C). Using a similar mechanism with a microarray device operating at 20 V peak-to-peak and 10 kHz, Sonnenberg *et al.*<sup>100</sup> separated DNA from blood cells, where high molecular weight DNA and nanoparticles were concentrated into high-field regions by positive DEP, while the blood cells were concentrated into the low-field regions by negative DEP. With this method, high molecular weight DNA could be detected at 260 ng/mL, a suitable range for DNA biomarkers (Figure 4D–F). Krishnan *et al.*<sup>101</sup> demonstrated separation of 10 nm polystyrene nanoparticles, 60 nm DNA-derivatized nanoparticles, and 200 nm nanoparticles. They demonstrated the feasibility of this technique even in physiological solutions with high conductance.

Besides isolation, nanoparticles can also be enriched through a mechanism of DEP trapping.<sup>102–106</sup> Cheng *et al.*<sup>107</sup> developed electrode arrays to generate DEP forces and aggregate bacteria with silver nanoparticles. They used this method to rapidly identify bacteria from diluted blood with surface-enhanced Raman spectroscopy (SERS) (Figure 5A,B). Han *et al.*<sup>108</sup> superimposed alternating current DEP and electro-osmosis between two coplanar electrodes to concentrate bacteria, viruses, and proteins. They enriched nanometer-sized MS2 viruses and troponin I antibody proteins. Yeo *et al.*<sup>109</sup> removed the constraints of a microfluidic device and developed a dendritic, multiterminal nanotip (*i.e.*, dendritic nanotip) for DEP-based concentration of viral particles. They showed that the dendritic nanotip could detect T7 phage as low as  $10^4$  particles per mL (20 particles in 2  $\mu$ L sample volume) in 5 min (Figure 5C,D).

Microfluidic DEP features several advantages.<sup>88,90,110,111</sup> First, DEP forces do not require the target particles to carry a charge; it can work with both charged and neutral nanoparticles. Second, DEP forces require a nonuniform electric field, which can be easily achieved with modern microfluidic designs and electrode fabrication techniques. In addition, the laminar flow nature in microfluidic channels provides superior flow control over bulk devices. However, microfluidic DEP has several limitations that still need to be addressed. First, despite the wide application of DEP-based approaches, its underlying mechanism is not yet fully understood. The dielectric properties of the material, angular frequency of the applied electric field, and the charge and size of the particles all affect the separation results.<sup>90</sup> Therefore, it is not straightforward to predict the performance of DEP separations

prior to separation experiments. Second, many DEP-based biological applications require a specific medium with a predefined conductivity, which can affect the biological functions of the targets. In addition, applying external voltages to drive particle motion might induce electrothermal flows and joule heating,<sup>112</sup> which can disrupt the separation process and the integrity of biological nanoparticles.

## MICROFLUIDIC FILTRATION

Filtration is one of the most widely used industrial nanoparticle isolation methods in water treatment, which fractionizes nanoparticles with direct physical barriers. Its microfluidic counterparts<sup>113–117</sup> are based on similar underlying concepts but are also designed to deal with samples with small volumes. Traditionally, microfluidic filtration is also categorized, at least in part, into field-flow fractionation,<sup>118</sup> which is defined by features of the flow field, rather than the nature of filtration. In this regard, asymmetric flow field-flow fractionation (AF4) products are commercially available for the separation of a wide spectrum of proteins, liposomes, emulsions, viruses, polysaccharides, metals, and polymeric nanoparticles.<sup>119–122</sup> Recently, Zhang *et al.*<sup>123</sup> used AF4 to identify two exosome subpopulations (large exosome vesicles of 90–120 nm and small exosome vesicles of 60–80 nm) and discovered an abundant population of nonmembranous nanoparticles termed “exomers” (~35 nm). Besides commercial systems, emerging concepts on microfluidic filtration are under rapid development. For example, Davies *et al.*<sup>124</sup> developed a microfluidic filtration system with porous polymer monolithic membranes in poly(methyl methacrylate) microfluidic chips by UV photopolymerization to isolate vesicles from whole blood samples. The filtration was driven by pump injection or DC electrophoresis. Liang *et al.*<sup>125</sup> developed a double-filtration microfluidic device that isolated and enriched extracellular vesicles with a size range of 30–200 nm from urine. They demonstrated an isolation yield of 80% in isolating extracellular vesicles from T24 cell culture and urine samples (Figure 6A,B) and applied their method to the detection of bladder cancer. We do not discuss nanoparticle enrichment based on filtration because isolation through filtration is typically also an enriching process.

As a direct derivative of filtration, microfluidic filtration shares some of the same intrinsic limitations which researchers are devoting efforts to overcome. For example, nanoparticles moving through a nanoporous filter usually require high energy and might block or clog the membrane. To address both issues, Ang *et al.*<sup>126</sup> use surface acoustic waves (SAW) to enhance transport through graphene films. They achieved 100% filtration efficiency for microscale particles, 95% for the filtration of particles as small as tens of nanometers in diameter and demonstrated the ability to separate nanoparticles with diameters of 25 and 50 nm. To circumvent clogging of the membrane, a backwash was applied to flush the incorporated nanoparticles simply by reversing the SAW-induced flow. A filtration efficiency of 98% was achieved after SAW-induced backwash (Figure 6C,D). Another limitation for filtration is that once a membrane is prepared, the pore size is difficult to change. To overcome this limitation, Haefner *et al.*<sup>127</sup> demonstrated a method to adapt the size exclusion functionality of poly-*N*-isopropylacrylamide (PNIPAAm)-based nano/microfilters in 2D and 3D microfluidic systems. The pore size can be adjusted from nanometers to micro-meters by shrinking or swelling in response to organic solvents.



## MICROFLUIDIC DETERMINISTIC LATERAL DISPLACEMENT (DLD)

Microfluidic DLD utilizes the arrangement of pillars to control the trajectory of particles, thus facilitating the separation of particles larger and smaller than a critical diameter.<sup>128,129</sup> DLD offers superior size resolutions for nanoparticle isolation. For example, Huang *et al.*<sup>130</sup> isolated microspheres of 0.8, 0.9, and 1.0  $\mu\text{m}$  in 40 s with a resolution of  $\sim 10$  nm at a flow speed of approximately 100  $\mu\text{m}/\text{s}$ . They also succeeded in separating large bacterial DNA with sizes ranging from 1000 to 600 nm (Figure 7A,B). Later, Santana *et al.*<sup>131</sup> used DLD to separate cancer-cell-derived (BxPC-3 cells) extracellular vesicles; they demonstrated a yield of 39% with a corresponding purity of 98.5% in target output. Although the yield is less than optimal, the high purity can potentially benefit downstream cancer diagnostic applications. Since established, researchers have worked on improving the performance of DLD for nanoparticle isolation. First, researchers enabled the isolation of nanoparticles with smaller sizes by creating a “Nano-DLD”. Wunsch *et al.*<sup>132</sup> used manufacturable silicon to produce nanoscale DLD with uniform gap sizes ranging from 25 to 235 nm. They demonstrated the separation of nanoparticles between 20 and 110 nm based on size; they also separated exosomes based on their sizes (average 60–80 nm, ranging from 20 to 140 nm), a necessary precursor for single-particle exosome analysis (Figure 7C,D). In addition, researchers enhance the dynamic range for nanoparticles in DLD separation by actively manipulating the particle size. For example, by altering the ionic concentrations of various buffer solutions, Zeming *et al.*<sup>133</sup> are able to modulate the effective size of nanoparticles. This in turn changes the magnitude of the electrostatic force between the nanoparticles and the walls of the DLD device (Figure 7E). They demonstrated dynamic control of the separation spectrum, which ranged from 51 to 1500 nm, in a continuous flow matter; this separation spectrum is  $\sim 12$  times larger than that of conventional DLD separation.

Although primarily used for isolation, DLD is also utilized for nanoparticle enrichment. It is based on the mechanism of nanoparticle focusing in pillar arrays. For example, Chen *et al.*<sup>134</sup> reported an increase of DNA (diameter of  $\sim 250$  nm) concentration by a factor of 87, with a throughput of 0.25  $\mu\text{L}/\text{h}$  (at 40  $\mu\text{m}/\text{s}$  flow velocity). Particularly, they increased the shear modulus and compacted the DNA molecules using polyethylene glycol (PEG, 10% w/v) to enhance separation performance. They claimed that the purification of DNA from enzymatic reactions can be integrated to produce next-generation DNA sequencing libraries.

DLD methods possess the characteristics of robust isolation performance, high resolution, and elimination of external forces for nanoparticle isolation and enrichment. Incorporating pillar structures into a microfluidic device allows precise control over interactions between particles, flows, and microstructures. However, current DLD methods still suffer from some intrinsic limitations: first, fluid volumes processed by DLD are typically very small (1–10  $\mu\text{L}/\text{min}$ ). Second, devices can be easily clogged by larger particles and impurities. To circumvent the first limitation, DLD nanoparticle separation is primarily used in diagnostic purposes for extracellular vesicles and DNAs, where throughput is not a primary concern due to the high concentration of biomarkers. To address the second concern, DLD devices can be integrated with other mechanisms to pretreat samples and remove larger objects that may clog the device.

## INERTIAL MICROFLUIDICS

Inertial microfluidic<sup>135–140</sup> approaches for nanoparticle isolation utilize the inertial migration of particles in a microfluidic channel with predesigned shapes (*e.g.*, straight channel, spiral channel, or wavy channel) and cross-sectional geometries (*e.g.*, rectangular, circular, or triangular) to focus nanoparticles at different positions. The effect of inertial focusing effect is driven by the shear-gradient lift and wall effect lift and is dependent on the design of the channel, the flow rates, and the size of the particle.<sup>141</sup> Thus, inertial focusing is able to isolate nanoparticles with various sizes. In this regard, Bhagat *et al.*<sup>142</sup> demonstrated the extraction of 590 nm polystyrene particles from a mixture of 1.9  $\mu\text{m}$  and 590 nm particles in a straight microfluidic channel with rectangular cross section (Figure 8A,B).

To better control the particle trajectories in microfluidic channels, polymers were introduced as the suspending liquid to carry nanoparticles. Particles, driven by the elastic force generated by the deformation of the polymer chains, migrate transverse to the flow direction, achieving “viscoelastic focusing”.<sup>141</sup> Using viscoelastic focusing in nanoparticle isolation, Liu *et al.*<sup>143</sup> used spiral microfluidic devices to separate binary mixtures of 100 and 2000 nm polystyrene particles and  $\lambda$ -DNA molecules/blood platelets in solution of poly(ethylene oxide). They achieved a separation efficiency of >95%. Liu *et al.*<sup>144</sup> designed a channel with a high-aspect-ratio cross section with a height of 50  $\mu\text{m}$  and width of 20  $\mu\text{m}$ ; exosomes were isolated from cell culture media with a high separation purity (>90%) and yield (>80%) of exosomes. They also demonstrated the separation of 100 and 500 nm polystyrene nanoparticles. They could change the cutoff size of nanoparticles by tuning the viscoelasticity of the suspending medium by changing the concentration of poly(ethylene oxide). Wang *et al.*<sup>145</sup> further optimized the wavy channel design and used thermoset polyester to replace polydimethylsiloxane (PDMS). By doing this, they reduced the pressure-induced deformation of the channel cross section and maintained the focusing effect at larger flow rates up to 1400  $\mu\text{L}/\text{min}$ . They demonstrated a separation between 920 and 200 nm polystyrene microspheres, although the separation performance at this condition needs further characterization (Figure 8C).

Nanoparticles can also be enriched in the microchannel through the inertial focusing and viscoelastic focusing.<sup>138,140</sup> Kim *et al.*<sup>146</sup> designed a straight channel with a rectangular cross section, and they used it to focus fluorescent submicron polystyrene beads with 500 and 200 nm diameters along the central line of a microchannel with the addition of 500 ppm poly(ethylene oxide). They also focused flexible DNA molecules ( $\lambda$ -DNA and T4-DNA), which have radii of gyration ( $R_g$ ) of approximately 0.69 and 1.5 nm, respectively. Zhou *et al.*<sup>147</sup> integrated the processes of focusing and isolation of exosomes into one device (Figure 9). They periodically reversed the Dean secondary flow that is generated by repeated wavy channel structures, causing bigger particles (*e.g.*, large extracellular vesicles) to be focused in the central line and smaller particles (*e.g.*, exosomes) to be focused along the edge for separation. They achieved an exosome purity of 92.8% after one single separation process.

Compared with methods that utilize external forces such as optics, acoustics, or electronics, inertial microfluidic nanoparticle isolation and enrichment techniques possess advantages



in terms of their ease of use, lack of requirements for external actuation, and robust performance once operational parameters are optimized. Compared with DLD methods, the removal of pillars avoids concerns over channel clogging and increases the throughput. A microfluidic channel also enabled precise fluid control over capillary number, Reynolds number, and Peclet number,<sup>135</sup> which is challenging in bulk devices. Nonetheless, inertial microfluidic operation often works at high flow rates, where the shear might cause potential damage to biological nanoparticles. Although there are no reports studying this effect in detail, further validation might be necessary in order to confirm the biocompatibility of inertial techniques.

## OPTOFLUIDICS

Integrating optics with microfluidics (*i.e.*, optofluidics)<sup>148–153</sup> provides a powerful tool to isolate and enrich nanoparticles with high resolution.<sup>154–161</sup> Nan *et al.*<sup>162</sup> isolated metal nanoparticles with dynamic and tunable optical forces generated by phase gradients of light. Size-dependent optical forces drive nanoparticles of different sizes with different velocities in solution, leading to their separation. They demonstrated the separation of silver and gold nanoparticles in the diameter range of 70–150 nm with a resolution down to 10 nm. Particle separation was conducted in static flow conditions (Figure 10A,B). Shilkin *et al.*<sup>163</sup> used high-quality Mie resonances to exert optical forces on spherical silicon nanoparticles for size-based nanoparticle separation. They resolve nanoparticles of diameters 130, 150, and 160 nm, resulting in a resolution of 10 nm. The separation was also conducted in static flow conditions (Figure 10C,D). To increase throughput, Wu *et al.*<sup>164</sup> combined optical and hydrodynamic forces to separate gold nanoparticles in a flowing system (Figure 10E,F). They demonstrated the separation of gold nanoparticles with diameters of 50 vs 100 nm and 100 vs 200 nm. The sorting purities are 92% for the 50/100 nm combination and 86% for the 100/200 nm set, with a throughput of 300 particles/min. The throughput is much higher than those conducted in static conditions. They also reported a successful nanoparticle separation with smaller heterogeneity (*i.e.*, 50 vs 70 nm). In addition to dealing with “hard” nanoparticles (*e.g.*, Ag and Au), researchers also attempted to sort “soft” particles with stiffnesses ranging from  $10^{-10}$  to  $10^{-8}$  N/m (*e.g.*, polymers, viruses, and DNAs). Shi *et al.*<sup>165</sup> synchronized the optical force and drag force to separate 100 and 150 nm polystyrene nanoparticles with single nanometer precision.

Optical methods have also been applied to enrich nanoparticles, which is usually achieved through a laser-induced thermophoretic effect.<sup>166–169</sup> For example, Weinert *et al.*<sup>170</sup> used laser-induced bidirectional flow combined with a perpendicular thermophoretic molecule drift to concentrate biological nanoparticles (Figure 11A,B). They demonstrated the accumulation of a hundredfold excess of 5-base DNA within seconds and polystyrene nanoparticles with 40 nm diameters. Later, Yu *et al.*<sup>171</sup> reported a laser thermophoresis-based method to detect DNA (Figure 11C,D). They concentrate both DNA-functionalized gold nanoparticles and fluorescent DNA probes to capture target DNA in free solution. Once DNA and probes are bonded, the thermophoretic properties of the fluorescent probes changed. Their work shed a light on detecting DNA in serum-containing buffers without any channel, pump, or washing steps. The thermophoretic effect can be controlled more precisely with plasmonic structures.<sup>172–174</sup> For example, Braun *et al.*<sup>175</sup> created

nanostructures by depositing gold films on glass cover slides, which acted as microscopic heat sources to generate localized temperature gradients. They were able to enrich 200 nm nanoparticles at a predefined position *via* localized thermophoretic trapping.

Optofluidic methods are especially suitable for manipulating nanoparticles. First, the interaction of light and nanoparticles provides a wide spectrum of forces to drive the motion of nanoparticles. Those forces include, but are not limited to, scattering and gradient forces, surface plasmon resonance, and thermal-hydrodynamic forces. Second, light has great directionality and can be controlled precisely by tuning the wavelength, power, and duration, which enables high-resolution nanoparticle separations. Reported optical methods can isolate nanoparticles with a 10 nm resolution, which is very difficult to achieve through other mechanisms. Third, optical methods are convenient to integrate into microfluidic devices. Nonetheless, separation of nanoparticles by light also suffers some theoretical and practical challenges: (1) Since light can interact with nanoparticles in various ways, the performance of separation is difficult to predict for each type of nanoparticle. For example, the studies we discussed earlier are all based on single material systems (*e.g.*, Ag or Au); however, once the material changes, the separation performance can be drastically different. (2) Most current reports are based on metallic or silicon particles. When separating biological nanoparticles, the biocompatibility is a concern since the medium might absorb the energy from the light and convert it into heat.

## ELECTROPHORESIS

Nanoparticles that have different charges can be readily isolated and enriched with microfluidic electrophoresis.<sup>176–180</sup> The mechanism of microfluidic electrophoresis is similar to that in conventional gel electrophoresis<sup>181,182</sup> or capillary electrophoresis,<sup>183</sup> which is based on differences in the electrophoretic mobility of solutes (*e.g.*, zeta-potential<sup>176</sup> and size). Electrophoresis has been widely used in separating nanoparticles such as inorganic nanoparticles, proteins, peptides, and DNAs.<sup>184,185</sup> Using microfluidic devices allows for a greater amount of flexibility in the spatial configurations of the electrical field and sample flow. Sun *et al.*<sup>186</sup> used a free-flow microfluidic electrophoresis chip to separate a mixture of FITC-BSA, FITC-lysozyme, and FITC-pepsin based on their charges and/or sizes. Jeon *et al.*<sup>187</sup> separated molecular dyes of BODIPY<sup>2-</sup> and PTS<sup>4-</sup> with microfluidic electrophoresis based on the charge differences. Interestingly, electrophoretic methods were also used to isolate nanoparticles with differences in shape. For example, Hanauer *et al.*<sup>188</sup> demonstrated the separation of gold and silver nanoparticles according to their size and shape by agarose gel electrophoresis after coating nanoparticles with a charged polymer layer. They used color, a shape-dependent optical property of gold and silver nanoparticles, to validate the separation effect. They also demonstrated the capability of shape-dependent separation by separating silver rods with aspect ratios (length/width) of  $8.3 \pm 0.8$  vs  $3.1 \pm 0.7$ .

Electrophoretic methods have been extensively used for nanoparticle separations. They have several advantages. First, the electrophoretic force does not decay cubically with particle diameter (it is linear with the particle diameter);<sup>187,189</sup> therefore, the electrophoresis-based methods can maintain high performance even for particles at the nanoscale. Second, it is

able to conveniently separate peptides and proteins. Because the charges of peptides and proteins usually change with pH, isoelectric focusing<sup>190,191</sup> can be utilized to move the molecules in the presence of a pH gradient until the net charge of the molecule is zero (*i.e.*, isoelectric point). Third, electrophoretic methods can be used to separate nanoparticles with surface modifications. nanoparticle surface modification is a critical step to adjust surface properties, which is important for catalysis and biomedicine.<sup>192–194</sup> As an example of separating nanoparticles with different surface properties, Wang *et al.*<sup>195</sup> used capillary electrophoresis to monitor changes in the surface ligands of quantum dots. Integrating electrophoretic separation into microfluidic devices allows more precisely controlling the flow and electrodes over bulk operations. On the other hand, microfluidic electrophoresis generates Joule heating<sup>112</sup> and might cause bubble generation,<sup>196</sup> both of which can be damaging to biological samples and hinder consistent device performance. Researchers have developed flow-induced electrophoresis,<sup>187</sup> buffer additives,<sup>197</sup> and insulating wall<sup>198</sup> structures to circumvent these limitations.

## MICROFLUIDIC AFFINITY ISOLATION

Certain biological nanoparticles (*e.g.*, virus and exosomes) can be isolated based on specific antigens that are expressed on their surface using target antibodies. Microfluidic affinity-based nanoparticle separation has been studied extensively to enrich extracellular vesicles from various biological matrices. Chen *et al.*<sup>199</sup> reported a microfluidic exosome capture device, which employed an anti-CD63 modified microfluidic channel. Herringbone structures were fabricated on the ceiling of the microchannel to enhance capture efficiency. Compared to conventional ultracentrifugation, the microfluidic affinity capture method shortens the sample processing time and eliminates the need for expensive instruments. Kanwar *et al.*<sup>200</sup> fabricated an exosome capture device with circular wide channels that were interconnected with narrow fluid channels to promote the interaction between exosomes and surface-immobilized exosomes (Figure 12A,B). Exosomes captured by the device are examined using fluorescence microscopy or recovered for off-chip RNA analysis. Lo *et al.*<sup>201</sup> employed micropost structures to enhance the capture of exosomes in microfluidic channels. Desthiobiotin-conjugated antibodies were used as the capture antibodies, enabling the release of exosomes after capture. In addition to the channel geometry, channel surface properties are critical to the performance of affinity-based separation. Zhang *et al.*<sup>202</sup> developed a method of coating graphene oxide and polydopamine to form nanostructures on the channel surface (Figure 12C). This coating improves exosome capture while reducing nonspecific binding. An exosome ELISA assay based on this strategy achieved a limit of detection of  $50 \mu\text{L}^{-1}$  with a 4 order of magnitude dynamic range. To further improve the detection sensitivity of exosomes, combining herringbone structures with nanoscale features on the channel surface have been demonstrated to be effective.<sup>203,204</sup> Recently, Zhang *et al.* fabricated nanopatterns on the surface of herringbone structures through a self-assembly process, achieving a limit of detection of 10 exosomes/ $\mu\text{L}$ .<sup>204</sup> In addition, affinity-based isolation devices are generally amenable to the integration of detection function units. He *et al.*<sup>205</sup> reported an integrated exosome separation and intravesicular protein analysis based on two-stage immunomagnetic captures. The first stage isolates exosomes using antibody modified magnetic beads. After on-chip lysis, the second-stage

immunomagnetic separation allows for the isolation of target intravesicular proteins for ELISA analysis. Im *et al.*<sup>206</sup> combined surface plasmon resonance with affinity capture to achieve multiplexed detection of exosomes for a panel of protein markers. Jeong *et al.*<sup>207</sup> combined immunomagnetic capture and electrochemical detection to develop a portable and integrated exosome separation and detection device for studying exosomes in plasma samples from ovarian cancer patients (Figure 12D). In addition to exosomes, Wang *et al.*<sup>208</sup> developed a microfluidic affinity capture device to isolate subtypes of HIV using an anti-gp120 modified channel surface. A capture efficiency of 75% was achieved for spiked human blood samples.

Affinity-based separation allows researchers to isolate phenotypically pure biological nanoparticles from a mixture of background particles, which can provide more relevant results for biologists as compared to physical property-based methods. Conventionally, affinity separation is typically performed with antibody-labeled magnetic particles or affinity-based chromatography. To date, many microfluidic affinity separation methods have been reported to possess advantages over conventional methods. First, microfluidics can control the fluid profile and shear stress precisely, enabling optimal separation conditions to maximize capture efficiency while maintaining low levels of nonspecific binding. Second, microfluidic devices offer large surface-to-volume ratios, which promotes the interaction between particles and the affinity surface, thereby improving the capture efficiency. Third, affinity separation microdevices can be integrated with upstream sample preparation units and downstream particle characterization units to streamline and simplify the entire nanoparticle isolation workflow. Nonetheless, design of affinity separation requires prior knowledge on the surface biochemical properties of nanoparticles.

## COMPARISONS BETWEEN BULK AND MICROFLUIDIC METHODS FOR NANOPARTICLE ISOLATION AND ENRICHMENT

Nanoparticles can be isolated and enriched with large-scale, bulk methods which are capable of processing large volumes of sample material. Applications such as water treatment<sup>209,210</sup> utilize bulk ultrafiltration<sup>114,211–213</sup> and reverse osmosis<sup>214,215</sup> techniques to remove nanoparticles (*e.g.*, ions and proteins) and microparticles (*e.g.*, bacteria and particles). Filtration,<sup>216–218</sup> centrifugation,<sup>219–222</sup> electrophoresis,<sup>52,223–225</sup> and chromatography<sup>226–229</sup> are well-established bulk methods for separating proteins and cellular components from liquid media and/or other micro/nanoscale objects. Although bulk methods can be robust in processing large volume samples, they can also be constrained in certain applications. First, bulk methods typically require a minimum sample volume to perform nanoparticle separations; however, in diagnosis or catalysis, obtaining such volumes from rare samples can be problematic. Second, bulk methods have difficulties maintaining uniform separation conditions across the whole separation unit. For example, due to differences in the electrophoretic mobilities of ions at the center and edges of the gel plate arising from nonuniform temperatures, a so-called “smiling effect” occurs in protein/DNA gel electrophoresis, impairing the separation performance.<sup>230</sup> Considering the small size of nanoparticles, along with the miniscule differences between subpopulations of nanoparticles, nonuniform separation conditions prevent high separation efficiencies from

being achieved. Therefore, while bulky methods are robust and well-established, there is a great need for smaller, more precise approaches for nanoparticles isolation and enrichment.

To address these limitations, microfluidic devices<sup>45,46,231–234</sup> can be effective.<sup>235</sup> With the miniaturization of separation units to the micrometer scale, microfluidics provides several advantages over bulky methods. First, it is easier to maintain a homogeneous force field and separation conditions at smaller length scales, which helps to achieve a higher separation performance (*e.g.*, better purity and yield). Second, microfluidics is advantageous in dealing with nanoparticles contained in small sample volumes, which is particularly suitable for diagnostic and catalytic applications. Third, microfluidics features compact devices which render them easy to integrate into existing nanoparticle workflows. By eliminating the need to transfer a sample between multiple units, process stability is improved, and batch-to-batch variability can be reduced. Nonetheless, we understand that microfluidics is not a “one-size-fits-all” solution for nanoparticle isolation and enrichment. For example, microfluidics shares the same theoretical limitations with bulky methods in dealing with small particles down to the nanometer scale and in certain applications, additional investments on devices and equipment are required.

## ADDRESS THEORETICAL CHALLENGES IN THE MICROFLUIDIC ISOLATION AND ENRICHMENT OF NANOPARTICLES

As we discussed above, microfluidic methods offer distinct advantages over their bulky, benchtop counterparts in terms of control over conditions of isolation and enrichment, minimal sample volume requirements, and compactness of the device. However, these methods still face challenges from both theoretical and experimental aspects. For example, a volume of literature suggests that size is currently the most dominant characteristics for nanoparticle isolation and enrichment,<sup>236</sup> where nanoparticles are fractionized by their size, and then particles with certain sizes are enriched for later analysis. This strategy has achieved great success when applied to microparticles and cells for the following reasons. First, size is the most straightforward characteristics, which can be readily confirmed with microscope imaging. Second, most driving forces used to deflect particles are proportional to particle volume; as a result, small differences in the diameters of particles result in significant differences in the amount of force exerted on those particles. Third, size-based separation usually requires minimal sample pretreatment (*e.g.*, labeling), which simplifies the isolation process.

Despite the success of microfluidic isolation and enrichment of microparticles,<sup>237–242</sup> simply migrating size-based methods to nanoparticles introduces several theoretical limitations. First, the driving force decreases quickly at the nanometer scale as compared with the micrometer scale. For example, the magnitude of the acoustic radiation force,<sup>68,72,243</sup> which drives nanoparticle deflections in acoustic isolation, is proportional to the particle volume; however, the drag force, which impedes particle motion, is proportional to the diameter of particles.<sup>243</sup> Therefore, particles with a 100 nm diameter experience 1/1000 of the radiation force, but 1/10 of the drag force compared to particles with 1  $\mu\text{m}$  diameter. As a result, deflecting 100 nm particles in laminar flow is much more difficult

than that of 1  $\mu\text{m}$  particles. Similar volume-proportional forces also govern DEP-based isolation.<sup>235,244</sup> In addition to the diminished driving force, the noise from Brownian motion<sup>245,246</sup> is not negligible for nanoparticles. Taken together, isolation and enrichment at the nanoscale are theoretically more challenging than their counterparts at the microscale. To overcome the diminished performance of size-based isolation and enrichment at the nanoscale, the following strategies are suggested for consideration.

### **Optimize Parameters for Isolation and Enrichment at the Nanoscale.**

Researchers are often tempted to extrapolate isolation and enrichment parameters from the microscale to the nanoscale. For example, researchers reduce the pore size in filtration,<sup>125</sup> shorten the wavelength in acoustics,<sup>247,248</sup> increase power input, redesign channel shapes,<sup>132</sup> flow rates,<sup>143</sup> and apply recirculation<sup>249,250</sup> for repeated isolation. However, to increase the power in optical and acoustic methods requires additional power supplies and cooling units. Recirculation, which effectively increases the path of particles under impact, increases the purity but impairs the yield. Although parameter optimization can result in additional challenges, it is typically one of the first considerations for improving the performance of nanoparticle isolation and enrichment methods.

### **Scale Down the Dimensions of the Device.**

Besides the aforementioned limitations arising from the nature of the driving forces, most microfluidic devices are still too large to manipulate nanoparticles. Thus, scaling microfluidic devices down to the nanofluidic scale can drastically improve performance for the isolation and enrichment of nanoparticles. For example, DLD has demonstrated its superior performance in separating microscale cells and particles. To apply DLD in nanoparticle isolations, researchers reduced the gaps between each pillar and switched the device material from PDMS to silicon to form nano-DLD that is able to separate nanoparticles below 100 nm in diameter.<sup>132</sup> In addition to nano-DLD, nanochannels are also considered; Huh *et al.*<sup>251</sup> demonstrated tunable nanochannels which are able to selectively sieve particles with approximately 20 nm quantum dots. Stavis *et al.*<sup>252</sup> developed a nanofluidic channel that had a maximum depth of 620 nm, a minimum depth of 80 nm, and an average step size of 18 nm, to sort a bimodal mixture of nanoparticles by nanofluidic size exclusion. They separated nanoparticles with diameters of 100 and 210 nm and claimed that the minimum difference in diameter can be as small as 18 nm. However, in order to scale down devices to the nanoscale, alternative materials (*e.g.*, PDMS in micro-DLD to silicon in nano-DLD) and fabrication techniques (*e.g.*, soft lithography to high-resolution photolithography) are needed. In addition, with further scaling to the nanofluidic range, interactions at molecular levels are not negligible, which introduces further complexity for particle manipulations.<sup>253–255</sup>

### **Dynamically Adjust the Size of Nanoparticles.**

Zeming *et al.*<sup>133</sup> used different NaCl ionic concentrations to adjust the Debye length of polystyrene beads, therefore adjusting the isolation effect in real time of their DLD devices. Their strategy can be extended to a variety of nanoparticles. For example, the size of biological nanoparticles (*e.g.*, DNAs and proteins) depends on biochemical factors of the surrounding environment (*e.g.*, pH and salt concentration).<sup>256</sup> Likewise, the



hydrodynamic radius of many synthesized nanoparticles also depends on surface interactions with molecules in the suspending medium.<sup>257</sup> Therefore, it is possible to control the surrounding environment to increase their size or magnify the size difference between two particles. However, this approach directly changes the size and isolation effect, and additional postisolation procedures to recover nanoparticles in their natural structure are required, which may affect the bioactivity of proteins or DNAs.

### **Develop Mechanisms Based on Different Chemical and Physical Properties.**

Biological nanoparticles such as DNAs, proteins, vesicles, and exosomes can be isolated and enriched, with affinity-based methods in a single step.<sup>199,203,205–207</sup> In this case, the pros and cons of affinity-based methods, size-based methods, and other mechanisms must be considered. Size-based operations are free of labeling, immune-binding, and washing steps but lack specificity compared with antibody-based operations. Other than size, shape-based mechanisms<sup>188,219,236</sup> might be a good alternative to size-based isolation. Shape is important for nanoparticle applications in catalysis since it determines the surface-area-to-volume ratio. Shape also plays an important role in the bioavailability of nanoparticles, where studies have demonstrated that cylindrical nanoparticles interact with cells very differently than spherical ones.<sup>258,259</sup> In addition, characterizing shape differences is as straightforward as that of size. Nonetheless, understanding how different shapes respond to force fields is not clear, which hinders shape-based nanoparticle separation and enrichment. For example, particles with the same volume but different shapes seem to have different forces of acoustofluidics and DEP,<sup>188,219,236</sup> unfortunately, the quantitative analysis on these forces is not straightforward.

## **CONSIDERATIONS FOR THE FUTURE DEVELOPMENT AND COMMERCIALIZATION OF MICROFLUIDIC NANOPARTICLE ISOLATION AND ENRICHMENT SYSTEMS**

Despite the numerous demonstrations of microfluidic nanoparticle isolation and enrichment, several aspects still need to be improved, including the specificity of application, ease of integration, and accessibility to end users.

### **Tailor Microfluidic Methods for Specific Applications.**

Due to the complex nature of nanoparticles, it is unlikely to have one mechanism that can be classified as a “one size fits all” approach. For example, separation methods that work best for metal nanoparticles may not be the optimal method for biological nanoparticles. Purification and enrichment of extracellular vesicles from various kinds of biological fluids has become increasingly important in recent years. Methods that target extracellular vesicles need to be tailored to accommodate the requirements and characteristics of extracellular vesicles.<sup>76,132,144,147,227</sup> For example, for certain applications, the integrity of extracellular vesicles needs to be preserved, which requires gentle separation mechanisms or mild separation procedures. In addition, to facilitate the characterization of protein or RNA contents of a vesicles,<sup>260–264</sup> a method needs to be capable of both enriching nanoparticles and exhibiting high compatibility with a wide range of biochemical characterization assays.

### **Develop Integrated Microfluidic Separation-Enrichment-Analysis Platforms.**

One of the advantages of microfluidic methods is the potential for integration with multiple working mechanisms or functional units. As an example of integrating different working mechanisms, acoustic and magnetic methods have been combined with surface affinity bindings to isolate and enrich exosomes.<sup>76</sup> Here, exosomes are specifically bonded onto microparticles through surface biomarkers for enrichment; then, an acoustic or magnetic field is applied to deflect bonded exosomes with free ones for isolation. In addition to integrating multiple working mechanisms to improve isolation performance, combining the nanoparticle isolation, enrichment, and characterization units into one system is expected to provide a “sample in-answer out” device. For example, Cheng *et al.*<sup>107</sup> demonstrated the enrichment of Ag nanoparticles with bacteria to facilitate SERS detection; Yu *et al.*<sup>171</sup> demonstrated the enrichment of probe-coated nanoparticles with DNAs for fluorescent detection; Yeo *et al.*<sup>104,109</sup> reported concentrating viruses onto nanotips for fluorescent and electron microscopy imaging detection.

### **Improve the Accessibility of Microfluidic Systems through Commercialization.**

Despite the great promise of microfluidic methods, ultracentrifugation is still the most widely used approach for nanoparticle isolation and enrichment despite concerns over its biocompatibility. This is largely because ultracentrifugation and other conventional methods are commercially available and have established operation protocols that even nonexperts on the instrumentation can perform. Most of the existing microfluidic methodologies are still at the proof-of-concept stage and must be performed by skilled personnel in microfluidics.<sup>46</sup> Many nonstandard device fabrication and operation procedures make microfluidic methods difficult to be adopted by other communities. Efforts should be made to improve device fabrication procedures and reduce the need for peripheral equipment. For example, the central components of microfluidic channels can be fabricated with materials of paper,<sup>265,266</sup> plastic,<sup>267,268</sup> or glass,<sup>43,55</sup> rather than PDMS, through standard industrial manufacturing processes. Ultimately, the broader impact of instrumentation comes from the commercialization of the instrument. In this regard, one example is the commercially available Eclipse AF4, which utilizes the flow field-flow fractionation for size-based separations of proteins, liposomes, virus, and other nanoparticles.<sup>119,121,123</sup> On the other hand, in resource-limited settings, developing point-of-care nanoparticle separation, enrichment, and characterization systems could be especially attractive for microfluidic-based methods. For example, Bachman *et al.*<sup>82</sup> developed an on-demand acoustofluidic pump and mixer by incorporating a cell phone, a Bluetooth speaker, a sharp-edge-based acoustofluidic device, and a simple portable microscope. They created a fully functional prototype with commercially available Arduino components that holds great potential for use in point-of-care applications.<sup>84</sup>

## **EMERGING MARKETS OF MICROFLUIDIC NANOPARTICLE ISOLATION AND ENRICHMENT IN BIOMEDICINE**

In this section, we provide our perspective on biological and medical applications of microfluidic nanoparticle isolation and enrichment. We will cover both fundamental research

in the study of membrane-bound and membrane-less organelles, as well as clinical diagnostics and therapeutics.

### Research on Membrane-Bound Organelles.

To date, a myriad of microfluidic methods for the isolation and enrichment of extracellular vesicles have been reported.<sup>76,132,144,147,227</sup> In addition to extracellular vesicles, there are many membrane-bound organelles with great significance for human health, such as those forming the mitochondria, secretory vesicles, endosomal and lysosomal system, peroxisomes, lipid droplets, autophagosomes.<sup>269</sup> These organelles are often nanometer-sized particles with a variety of transmembrane markers presenting for their vesicular trafficking and functions.<sup>269</sup> To study organelles' function, development, and use in diagnostics, methods to isolate and enrich these organelles are preferable. Although conventionally isolated and enriched by ultracentrifugation, these organelles are attainable targets for microfluidic methods, due to their nanoscale size and enriched surface markers. In fact, microfluidic methods are expected to be advantageous compared to conventional ultracentrifugation because high-speed rotation (>100,000g in ultracentrifugation)<sup>270</sup> and the formation of centrifuge pellets might damage membrane-bound organelles and alter protein functions.

### Research on Membrane-Less Organelles.

Besides membrane-bound organelles, a number of cell compartments are membrane-less (*e.g.*, membrane-less organelles).<sup>271</sup> They lack the boundary of a lipid bilayers, exist usually transiently, and are formed *via* the mechanism of liquid-liquid phase separations.<sup>272</sup> Although current biological studies have revealed the importance of membrane-less compartments in neurodegenerative diseases,<sup>273,274</sup> stress responses,<sup>275</sup> and many other important physiological processes,<sup>271</sup> little has been reported on their isolation and enrichment due to technical challenges. For example, stress granules,<sup>276</sup> a membrane-less organelle of dense aggregations of proteins and RNAs that appears when the cell is under stress, are 100–200 nm in diameter. They have recently been isolated and collected with a multistep immune-affinity-based method.<sup>277</sup> Membrane-less organelles appear to be unsuitable for centrifugation because subjecting them to a strong centrifugal force may degrade them due to their lack of a membrane structure. In this regard, microfluidic methods are superior in handling these organelles as they can work under mild conditions, operate continuously to isolate “fresh” objects, and deal with small volume samples.

### Diagnosis of Diseases.

Nanoparticles have been extensively studied and widely applied in disease diagnostics. “Hard nanoparticles” (*e.g.*, gold) were conjugated with antibodies, enabling the binding and detection of protein biomarkers which are secreted from tumor cells.<sup>278</sup> Superparamagnetic nanoparticles were used as contrast agents to improve the resolution of magnetic resonance imaging.<sup>279</sup> On the other hand, “soft nanoparticles” (*e.g.*, exosomes and extracellular vesicles) have been utilized as a biomarker to diagnose cancer<sup>76</sup> and central nervous system diseases.<sup>280</sup> Isolation and enrichment of nanoparticles can benefit diagnostics in the following aspects. First, when using “hard nanoparticles” as probes for diagnostics, a procedure of isolation and enrichment can enhance the diagnostic performance because

the optical and magnetic responses are closely correlated with the size and shape of the nanoparticles. Second, the isolation and enrichment of “soft nanoparticles” provides possibility in disease diagnostics. Similar to exosomes, other membrane and membrane-less cellular organelles, isolated and enriched by microfluidic methods, can be a biomarker for diseases. In this regard, microfluidic methods are advantageous because they are capable of handling small volume samples that can be collected in a noninvasive manner. Using this approach, it is possible to develop point-of-care microfluidic devices for early stage disease diagnostics and treatment monitoring.

### From “Precise Medicine” to “Ultraprecise Nanomedicine”.

The interaction between medical nanoparticles and biological systems depends on the properties of the nanoparticles, including their size, shape, surface charge, surface roughness, and hydrophilicity/hydrophobicity.<sup>26,30,31,258,281</sup> These properties influence the specificity and toxicity of nanomedicines. To achieve “precise medicine”, material scientists have devised various strategies to improve the selectivity of nanoparticles<sup>282,283</sup> to a particular tissue or cell population. Microfluidic researchers are expected to make “ultraprecise nanomedicine” by adding nanoparticle isolation and enrichment steps to enhance the homogeneity of nanoparticles. For example, a better homogeneity in the size of nanoparticles may improve their circulation time in blood and tumor targeting ability. It is reported that nanoparticles with approximately 100 nm diameter favors for blood circulation and tumor accumulation *via* the enhanced permeability and retention effect;<sup>284</sup> on the other hand, nanoparticles with sizes less than 10 nm can cause genotoxic effects through point mutations, chromosomal fragmentation, and DNA strand breakages.<sup>285</sup> Taken together, impurities from small nanoparticles might lead to severe side effects during nanoparticle cancer therapy. However, nanoparticles fabricated by either bottom-up (*e.g.*, nucleation-growth) or top-down mechanisms (*e.g.*, sonication and fracturing) suffer from a wide size distribution. Separation methods will become a powerful tool to produce uniform nanoparticles, and enrichment methods will increase the concentration of target nanoparticles, thereby improving homogeneity, reducing unwanted side effects, and eventually enabling ultraprecise nanomedicine.

## CONCLUSION

Over the past several years, there has been a rapid expansion in the number of microfluidic techniques for the isolation and enrichment of nanoparticles. Various technologies, including acoustofluidics, dielectrophoresis, microfluidic filtration, deterministic lateral displacement, inertial microfluidics, optofluidics, electrophoresis, and microfluidic affinity isolation are discussed in this review article. As this review is intended for readers from diverse backgrounds, we provided an overview explaining the underlying mechanism behind multiple microfluidic approaches. The governing equations behind each method was well described in the following review papers on acoustofluidics,<sup>56–61,63,67,72</sup> DEP,<sup>88,90,93,96,111</sup> inertial microfluidics,<sup>135,136,141</sup> and DLD,<sup>128,129</sup> *etc.*

By providing insights into the benefits and drawbacks of each technique, we hope to equip researchers with the necessary information to choose the microfluidic approach that

is best suited for their research needs. Microfluidic methods possess many advantages over conventional, bulk methods, including the ability to maintain homogeneous separation conditions at smaller length scales to achieve a higher separation performance and the ability to process nanoparticles from small volume samples. In addition, microfluidic devices are compact devices which render them easy to integrate into existing nanoparticle workflows. The performance of microfluidic methods has been comprehensively validated with both soft nanoparticles (*e.g.*, DNAs, exosomes, and viruses) and hard nanoparticles (*e.g.*, metal and silicon nanoparticles) in laboratory settings. In the near future, due to increased commercialization efforts, we expect microfluidic technologies for nanoparticle isolation and enrichment to have a broader impact in both research and commercial settings. By making microfluidic technologies more widely available and easy to use for researchers from diverse backgrounds, many applications and research directions, such as investigations into the role of membrane-less organelles in various diseases, will be enabled.

## ACKNOWLEDGMENTS

We acknowledge support from the National Institutes of Health (R01GM132603, R01GM135486, UG3TR002978, R33CA223908, R01GM127714, and R01HD086325), United States Army Medical Research Acquisition Activity (W81XWH-18-1-0242), and National Science Foundation (ECCS-1807601).

## VOCABULARY

### **nanoparticle isolation**

a process that acts as a selective barrier allowing relatively free passage of one component in the mixture of nanoparticles, while retaining or deflecting other components

### **nanoparticle enrichment**

a procedure that is conducted to increase the concentration of specific nanoparticles for collection

### **soft nanoparticles**

naturally existing, organic nanoparticles such as proteins, DNAs, viruses, and exosomes

### **hard nanoparticles**

synthesized, inorganic nanoparticles such as gold, silver, and silicon

### **acoustofluidics**

an approach that integrates acoustic manipulation with microfluidic devices

### **optofluidics**

an approach that integrates optical manipulation with microfluidic devices

## REFERENCES

- (1). Gleiter H Nanostructured Materials: Basic Concepts and Microstructure. Acta Mater. 2000, 48, 1–29.
- (2). Guo Z; Tan L Fundamentals and Applications of Nanomaterials; Artech House: Boston, MA, 2009.

- (3). Singh AK Engineered Nanoparticles: Structure, Properties and Mechanisms of Toxicity; Elsevier: Amsterdam, 2016.
- (4). Astruc D Introduction: Nanoparticles in Catalysis. *Chem. Rev* 2020, 120, 461–463. [PubMed: 31964144]
- (5). Navalon S; Garcia H Nanoparticles for Catalysis. *Nanomaterials* 2016, 6, 123.
- (6). Park SJ; Taton TA; Mirkin CA Array-Based Electrical Detection of DNA with Nanoparticle Probes. *Science* 2002, 295, 1503–1506. [PubMed: 11859188]
- (7). Choi C; Choi MK; Hyeon T; Kim D-H Nanomaterial-Based Soft Electronics for Healthcare Applications. *ChemNanoMat* 2016, 2, 1006–1017.
- (8). Chan WCW Bio-Applications of Nanoparticles. Springer Science + Business Media; Landes Bioscience: New York, 2007.
- (9). De M; Ghosh PS; Rotello VM Applications of Nanoparticles in Biology. *Adv. Mater* 2008, 20, 4225–4241.
- (10). Choi HS; Frangioni JV Nanoparticles for Biomedical Imaging: Fundamentals of Clinical Translation. *Mol. Imaging* 2010, 9, 291–310. [PubMed: 21084027]
- (11). Salata O Applications of Nanoparticles in Biology and Medicine. *J. Nanobiotechnol* 2004, 2, 3.
- (12). Rosi NL; Mirkin CA Nanostructures in Biodiagnostics. *Chem. Rev* 2005, 105, 1547–1562. [PubMed: 15826019]
- (13). Gu Z; Biswas A; Zhao M; Tang Y Tailoring Nanocarriers for Intracellular Protein Delivery. *Chem. Soc. Rev* 2011, 40, 3638–3655. [PubMed: 21566806]
- (14). Mitragotri S; Anderson DG; Chen X; Chow EK; Ho D; Kabanov AV; Karp JM; Kataoka K; Mirkin CA; Petrosko SH; Shi J; Stevens MM; Sun S; Teoh S; Venkatraman SS; Xia Y; Wang S; Gu Z; Xu C Accelerating the Translation of Nanomaterials in Biomedicine. *ACS Nano* 2015, 9, 6644–6654. [PubMed: 26115196]
- (15). Pacardo DB; Ligler FS; Gu Z Programmable Nanomedicine: Synergistic and Sequential Drug Delivery Systems. *Nanoscale* 2015, 7, 3381–3391. [PubMed: 25631684]
- (16). Cao YC; Jin R; Mirkin CA Nanoparticles with Raman Spectroscopic Fingerprints for DNA and RNA Detection. *Science* 2002, 297, 1536–1540. [PubMed: 12202825]
- (17). Smith BR; Gambhir SS Nanomaterials for *in Vivo* Imaging. *Chem. Rev* 2017, 117, 901–986. [PubMed: 28045253]
- (18). Shi J; Zhu Y; Zhang X; Baeyens WRG; Garcia-Campana AM Recent Developments in Nanomaterial Optical Sensors. *TrAC, Trends Anal. Chem* 2004, 23, 351–360.
- (19). Kelly KL; Coronado E; Zhao LL; Schatz GC The Optical Properties of Metal Nanoparticles: The Influence of Size, Shape, and Dielectric Environment. *J. Phys. Chem. B* 2003, 107, 668–677.
- (20). Albanese A; Tang PS; Chan WC The Effect of Nanoparticle Size, Shape, and Surface Chemistry on Biological Systems. *Annu. Rev. Biomed. Eng* 2012, 14, 1–16. [PubMed: 22524388]
- (21). Lockman PR; Mumper RJ; Khan MA; Allen DD Nanoparticle Technology for Drug Delivery across the Blood-Brain Barrier. *Drug Dev. Ind. Pharm* 2002, 28, 1–13. [PubMed: 11858519]
- (22). Saraiva C; Praca C; Ferreira R; Santos T; Ferreira L; Bernardino L Nanoparticle-Mediated Brain Drug Delivery: Over-coming Blood-Brain Barrier to Treat Neurodegenerative Diseases. *J. Controlled Release* 2016, 235, 34–47.
- (23). Wohlfart S; Gelperina S; Kreuter J Transport of Drugs across the Blood-Brain Barrier by Nanoparticles. *J. Controlled Release* 2012, 161, 264–273.
- (24). Zhou Y; Peng Z; Seven ES; Leblanc RM Crossing the Blood-Brain Barrier with Nanoparticles. *J. Controlled Release* 2018, 270, 290–303.
- (25). Almeida JP; Chen AL; Foster A; Drezek R In Vivo Biodistribution of Nanoparticles. *Nanomedicine (London, U. K.)* 2011, 6, 815–835.
- (26). Duan X; Li Y Physicochemical Characteristics of Nanoparticles Affect Circulation, Biodistribution, Cellular Internalization, and Trafficking. *Small* 2013, 9, 1521–1532. [PubMed: 23019091]
- (27). Owens DE III; Peppas NA Opsonization, Biodistribution, and Pharmacokinetics of Polymeric Nanoparticles. *Int. J. Pharm* 2006, 307, 93–102. [PubMed: 16303268]



- (28). Alexis F; Pridgen E; Molnar LK; Farokhzad OC Factors Affecting the Clearance and Biodistribution of Polymeric Nanoparticles. *Mol. Pharmaceutics* 2008, 5, 505–515.
- (29). Tsoi KM; MacParland SA; Ma XZ; Spetzler VN; Echeverri J; Ouyang B; Fadel SM; Sykes EA; Goldaracena N; Kathis JM; Conneely JB; Alman BA; Selzner M; Ostrowski MA; Adeyi OA; Zilman A; McGilvray ID; Chan WC Mechanism of Hard-Nanomaterial Clearance by the Liver. *Nat. Mater* 2016, 15, 1212–1221. [PubMed: 27525571]
- (30). Zhao F; Zhao Y; Liu Y; Chang X; Chen C; Zhao Y Cellular Uptake, Intracellular Trafficking, and Cytotoxicity of Nanomaterials. *Small* 2011, 7, 1322–1337. [PubMed: 21520409]
- (31). Alkilany AM; Nagaria PK; Hexel CR; Shaw TJ; Murphy CJ; Wyatt MD Cellular Uptake and Cytotoxicity of Gold Nanorods: Molecular Origin of Cytotoxicity and Surface Effects. *Small* 2009, 5, 701–708. [PubMed: 19226599]
- (32). Pan Y; Neuss S; Leifert A; Fischler M; Wen F; Simon U; Schmid G; Brandau W; Jahnke-Dechent W Size-Dependent Cytotoxicity of Gold Nanoparticles. *Small* 2007, 3, 1941–1949. [PubMed: 17963284]
- (33). Lewinski N; Colvin V; Drezek R Cytotoxicity of Nanoparticles. *Small* 2008, 4, 26–49. [PubMed: 18165959]
- (34). Nel A; Xia T; Madler L; Li N Toxic Potential of Materials at the Nanolevel. *Science* 2006, 311, 622–627. [PubMed: 16456071]
- (35). Aillon KL; Xie Y; El-Gendy N; Berkland CJ; Forrest ML Effects of Nanomaterial Physicochemical Properties on *in Vivo* Toxicity. *Adv. Drug Delivery Rev* 2009, 61, 457–466.
- (36). Zhu M; Nie G; Meng H; Xia T; Nel A; Zhao Y Physicochemical Properties Determine Nanomaterial Cellular Uptake, Transport, and Fate. *Acc. Chem. Res* 2013, 46, 622–631. [PubMed: 22891796]
- (37). Champion JA; Katare YK; Mitragotri S Particle Shape: A New Design Parameter for Micro- and Nanoscale Drug Delivery Carriers. *J. Controlled Release* 2007, 121, 3–9.
- (38). Mitragotri S In Drug Delivery, Shape Does Matter. *Pharm. Res* 2009, 26, 232–234. [PubMed: 18923811]
- (39). Yoo JW; Mitragotri S Polymer Particles that Switch Shape in Response to a Stimulus. *Proc. Natl. Acad. Sci. U. S. A* 2010, 107, 11205–11210. [PubMed: 20547873]
- (40). Seader JD; Henley EJ Separation Process Principles; Wiley: New York, 1998.
- (41). Geankoplis CJ Transport Processes and Separation Process Principles, 5th ed.; Prentice Hall: Boston, MA, 2018.
- (42). McCabe WL; Smith JC; Harriott P Unit Operations of Chemical Engineering, 7th ed.; McGraw-Hill: Boston, MA, 2005.
- (43). Mao Z; Li P; Wu M; Bachman H; Mesyngier N; Guo X; Liu S; Costanzo F; Huang TJ Enriching Nanoparticles via Acoustofluidics. *ACS Nano* 2017, 11, 603–612. [PubMed: 28068078]
- (44). Price CA; Eikenberry EF Centrifugation in Density Gradients; Academic Press: New York, 1982.
- (45). Squires TM; Quake SR Microfluidics: Fluid Physics at the Nanoliter Scale. *Rev. Mod. Phys* 2005, 77, 977–1026.
- (46). Whitesides GM The Origins and the Future of Microfluidics. *Nature* 2006, 442, 368–373. [PubMed: 16871203]
- (47). Cavazzini A; Pasti L; Massi A; Marchetti N; Dondi F Recent Applications in Chiral High Performance Liquid Chromatography: A Review. *Anal. Chim. Acta* 2011, 706, 205–222. [PubMed: 22023854]
- (48). Merken HM; Beecher GR Measurement of Food Flavonoids by High-Performance Liquid Chromatography: A Review. *J. Agric. Food Chem* 2000, 48, 577–599. [PubMed: 10725120]
- (49). Nahar L; Onder A; Sarker SD A Review on the Recent Advances in HPLC, UHPLC and UPLC Analyses of Naturally Occurring Cannabinoids (2010–2019). *Phytochem. Anal* 2020, 31, 413–457. [PubMed: 31849137]
- (50). Novakova L; Vlckova H A Review of Current Trends and Advances in Modern Bio-Analytical Methods: Chromatography and Sample Preparation. *Anal. Chim. Acta* 2009, 656, 8–35. [PubMed: 19932811]

- (51). Orlandini S; Gotti R; Furlanetto S Multivariate Optimization of Capillary Electrophoresis Methods: A Critical Review. *J. Pharm. Biomed. Anal* 2014, 87, 290–307. [PubMed: 23669025]
- (52). Zhu Z; Lu JJ; Liu S Protein Separation by Capillary Gel Electrophoresis: A Review. *Anal. Chim. Acta* 2012, 709, 21–31. [PubMed: 22122927]
- (53). Trojanowicz M Recent Developments in Electrochemical Flow Detections-a Review: Part I. Flow Analysis and Capillary Electrophoresis. *Anal. Chim. Acta* 2009, 653, 36–58. [PubMed: 19800474]
- (54). Landers JP Handbook of Capillary and Microchip Electrophoresis and Associated Microtechniques, 3rd ed.; CRC Press: Boca Raton, FL, 2008.
- (55). Harrison DJ; Fluri K; Seiler K; Fan Z; Effenhauser CS; Manz A Micromachining a Miniaturized Capillary Electrophoresis-Based Chemical Analysis System on a Chip. *Science* 1993, 261, 895–897. [PubMed: 17783736]
- (56). Ding X; Li P; Lin SC; Stratton ZS; Nama N; Guo F; Slotcavage D; Mao X; Shi J; Costanzo F; Huang TJ Surface Acoustic Wave Microfluidics. *Lab Chip* 2013, 13, 3626–3649. [PubMed: 23900527]
- (57). Ozcelik A; Rufo J; Guo F; Gu Y; Li P; Lata J; Huang TJ Acoustic Tweezers for the Life Sciences. *Nat. Methods* 2018, 15, 1021–1028. [PubMed: 30478321]
- (58). Mei JY; Friend J A Review: Controlling the Propagation of Surface Acoustic Waves via Waveguides for Potential Use in Acoustofluidics. *Mech Eng. Rev* 2020, 7, 19–00402.
- (59). Huang TJ Acoustofluidics: Merging Acoustics and Microfluidics for Biomedical Applications. *J. Acoust. Soc. Am* 2019, 145, 1786–1786.
- (60). Bose N; Zhang XL; Maiti TK; Chakraborty S The Role of Acoustofluidics in Targeted Drug Delivery. *Biomicrofluidics* 2015, 9, 052609. [PubMed: 26339329]
- (61). Li P; Huang TJ Applications of Acoustofluidics in Bioanalytical Chemistry. *Anal. Chem* 2019, 91, 757–767. [PubMed: 30561981]
- (62). Connacher W; Zhang NQ; Huang A; Mei JY; Zhang S; Gopesh T; Friend J Micro/Nano Acoustofluidics: Materials, Phenomena, Design, Devices, and Applications. *Lab Chip* 2018, 18, 1952–1996. [PubMed: 29922774]
- (63). Bruus H; Dual J; Hawkes J; Hill M; Laurell T; Nilsson J; Radel S; Sadhal S; Wiklund M Forthcoming Lab on a Chip Tutorial Series on Acoustofluidics: Acoustofluidics-Exploiting Ultrasonic Standing Wave Forces and Acoustic Streaming in Microfluidic Systems for Cell and Particle Manipulation. *Lab Chip* 2011, 11, 3579–3580. [PubMed: 21952310]
- (64). Fu YQ; Luo JK; Nguyen NT; Walton AJ; Flewitt AJ; Zu XT; Li Y; McHale G; Matthews A; Iborra E; Du H; Milne WI Advances in Piezoelectric Thin Films for Acoustic Biosensors, Acoustofluidics and Lab-on-Chip Applications. *Prog. Mater. Sci* 2017, 89, 31–91.
- (65). Friend J; Yeo LY Microscale Acoustofluidics: Microfluidics Driven via Acoustics and Ultrasonics. *Rev. Mod. Phys* 2011, 83, 647–704.
- (66). Xie YL; Bachman H; Huang TJ Acoustofluidic Methods in Cell Analysis. *TrAC, Trends Anal. Chem* 2019, 117, 280–290.
- (67). Bruus H Acoustofluidics: Theory and Simulation of Streaming and Radiation Forces at Ultrasound Resonances in Microfluidic Devices. *J. Acoust. Soc. Am* 2009, 125, 2592–2592.
- (68). Baasch T; Pavlic A; Dual J Acoustic Radiation Force Acting on a Heavy Particle in a Standing Wave Can Be Dominated by the Acoustic Microstreaming. *Phys. Rev. E: Stat. Phys., Plasmas, Fluids, Relat. Interdiscip. Top* 2019, 100, 061102.
- (69). Wu MX; Chen CY; Wang ZY; Bachman H; Ouyang YS; Huang PH; Sadovsky Y; Huang TJ Separating Extracellular Vesicles and Lipoproteins via Acoustofluidics. *Lab Chip* 2019, 19, 1174–1182. [PubMed: 30806400]
- (70). Wu MX; Ozcelik A; Rufo J; Wang ZY; Fang R; Huang TJ Acoustofluidic Separation of Cells and Particles. *Microsyst. Nanoeng* 2019, 5, 32. [PubMed: 31231539]
- (71). Wiklund M; Green R; Ohlin M Acoustofluidics 14: Applications of Acoustic Streaming in Microfluidic Devices. *Lab Chip* 2012, 12, 2438–2451. [PubMed: 22688253]
- (72). Bruus H Acoustofluidics 7: The Acoustic Radiation Force on Small Particles. *Lab Chip* 2012, 12, 1014–1021. [PubMed: 22349937]

- (73). Whitehill JD; Gralinski I; Joiner D; Neild A Nanoparticle Manipulation within a Microscale Acoustofluidic Droplet. *J. Nanopart. Res* 2012, 14, 1223.
- (74). Wu M; Mao Z; Chen K; Bachman H; Chen Y; Rufo J; Ren L; Li P; Wang L; Huang TJ Acoustic Separation of Nanoparticles in Continuous Flow. *Adv. Funct. Mater* 2017, 27, 1606039. [PubMed: 29104525]
- (75). Collins DJ; Alan T; Neild A Particle Separation Using Virtual Deterministic Lateral Displacement (VDLD). *Lab Chip* 2014, 14, 1595–1603. [PubMed: 24638896]
- (76). Wu M; Ouyang Y; Wang Z; Zhang R; Huang PH; Chen C; Li H; Li P; Quinn D; Dao M; Suresh S; Sadovsky Y; Huang TJ Isolation of Exosomes from Whole Blood by Integrating Acoustics and Microfluidics. *Proc. Natl. Acad. Sci. U. S. A* 2017, 114, 10584–10589. [PubMed: 28923936]
- (77). Lee K; Shao H; Weissleder R; Lee H Acoustic Purification of Extracellular Microvesicles. *ACS Nano* 2015, 9, 2321–2327. [PubMed: 25672598]
- (78). Collins DJ; Ma Z; Ai Y Highly Localized Acoustic Streaming and Size-Selective Submicrometer Particle Concentration Using High Frequency Microscale Focused Acoustic Fields. *Anal. Chem* 2016, 88, 5513–5522. [PubMed: 27102956]
- (79). Cui W; He M; Yang Y; Zhang H; Pang W; Duan X Hypersonic-Induced 3D Hydrodynamic Tweezers for Versatile Manipulations of Micro/Nanoscale Objects. *Part. Part. Syst. Charact* 2018, 35, 1800068.
- (80). Reyes C; Fu L; Suthanthiraraj PPA; Owens CE; Shields CW; López GP; Charbonneau P; Wiley BJ The Limits of Primary Radiation Forces in Bulk Acoustic Standing Waves for Concentrating Nanoparticles. *Part. Part. Syst. Charact* 2018, 35, 1700470.
- (81). Zhang LY; Tian ZH; Bachman H; Zhang PR; Huang TJ A Cell-Phone-Based Acoustofluidic Platform for Quantitative Point-of-Care Testing. *ACS Nano* 2020, 14, 3159–3169. [PubMed: 32119517]
- (82). Bachman H; Huang PH; Zhao SG; Yang SJ; Zhang PR; Fu H; Huang TJ Acoustofluidic Devices Controlled by Cell Phones. *Lab Chip* 2018, 18, 433–441. [PubMed: 29302660]
- (83). Zhao SG; Wu MX; Yang SJ; Wu YQ; Gu YY; Chen CY; Ye J; Xie ZM; Tian ZH; Bachman H; Huang PH; Xia JP; Zhang PR; Zhang HY; Huang TJ A Disposable Acoustofluidic Chip for Nano/Microparticle Separation Using Unidirectional Acoustic Transducers. *Lab Chip* 2020, 20, 1298–1308. [PubMed: 32195522]
- (84). Bachman H; Fu H; Huang PH; Tian ZH; Embry-Seckler J; Rufo J; Xie ZM; Hartman JH; Zhao SG; Yang SJ; Meyer JN; Huang TJ Open Source Acoustofluidics. *Lab Chip* 2019, 19, 2404–2414. [PubMed: 31240285]
- (85). Dash S; Mohanty S Dielectrophoretic Separation of Micron and Submicron Particles: A Review. *Electrophoresis* 2014, 35, 2656–2672. [PubMed: 24930837]
- (86). Karle M; Vashist SK; Zengerle R; von Stetten F Microfluidic Solutions Enabling Continuous Processing and Monitoring of Biological Samples: A Review. *Anal. Chim. Acta* 2016, 929, 1–22. [PubMed: 27251944]
- (87). Zhang C; Khoshmanesh K; Mitchell A; Kalantar-zadeh K Dielectrophoresis for Manipulation of Micro/Nano Particles in Microfluidic Systems. *Anal. Bioanal. Chem* 2010, 396, 401–420. [PubMed: 19578834]
- (88). Çetin B; Li D Dielectrophoresis in Microfluidics Technology. *Electrophoresis* 2011, 32, 2410–2427. [PubMed: 21922491]
- (89). Khoshmanesh K; Nahavandi S; Baratchi S; Mitchell A; Kalantar-zadeh K Dielectrophoretic Platforms for Bio-Microfluidic Systems. *Biosens. Bioelectron* 2011, 26, 1800–1814. [PubMed: 20933384]
- (90). Pethig R Dielectrophoresis: Status of the Theory, Technology, and Applications. *Biomicrofluidics* 2010, 4, No. 022811. [PubMed: 20697589]
- (91). Abdallah BG; Chao TC; Kupitz C; Fromme P; Ros A Dielectrophoretic Sorting of Membrane Protein Nanocrystals. *ACS Nano* 2013, 7, 9129–9137. [PubMed: 24004002]
- (92). Kentsch J; Durr M; Schnelle T; Gradl G; Muller T; Jager M; Normann A; Stelzle M Microdevices for Separation, Accumulation, and Analysis of Biological Micro- and Nanoparticles. *IEE Proc.: Nanobiotechnol* 2003, 150, 82–89. [PubMed: 16468936]

- (93). Neculae A; Biris CG; Bunoiu M; Lungu M Numerical Analysis of Nanoparticle Behavior in a Microfluidic Channel under Dielectrophoresis. *J. Nanopart. Res* 2012, 14, 1154.
- (94). Song YJ; Sonnenberg A; Heaney Y; Heller MJ Device for Dielectrophoretic Separation and Collection of Nanoparticles and DNA under High Conductance Conditions. *Electrophoresis* 2015, 36, 1107–1114. [PubMed: 25780998]
- (95). Jubery TZ; Srivastava SK; Dutta P Dielectrophoretic Separation of Bioparticles in Microdevices: A Review. *Electrophoresis* 2014, 35, 691–713. [PubMed: 24338825]
- (96). Cui HH; Voldman J; He XF; Lim KM Separation of Particles by Pulsed Dielectrophoresis. *Lab Chip* 2009, 9, 2306–2312. [PubMed: 19636460]
- (97). Voldman J Dielectrophoretic Traps for Cell Manipulation. In *Biomems and Biomedical Nanotechnology Vol. IV: Biomolecular Sensing, Processing and Analysis*, Ferrari M, Bashir R, Woreley S, Eds.; Springer US: Boston, MA, 2007; pp 159–186.
- (98). Viefhues M; Eichhorn R; Fredrich E; Regtmeier J; Anselmetti D Continuous and Reversible Mixing or Demixing of Nanoparticles by Dielectrophoresis. *Lab Chip* 2012, 12, 485–494. [PubMed: 22193706]
- (99). Zhao K; Peng R; Li D Separation of Nanoparticles by a Nano-Orifice Based Dc-Dielectrophoresis Method in a Pressure-Driven Flow. *Nanoscale* 2016, 8, 18945–18955. [PubMed: 27775139]
- (100). Sonnenberg A; Marciniak JY; Krishnan R; Heller MJ Dielectrophoretic Isolation of DNA and Nanoparticles from Blood. *Electrophoresis* 2012, 33, 2482–2490. [PubMed: 22899255]
- (101). Krishnan R; Sullivan BD; Mifflin RL; Esener SC; Heller MJ Alternating Current Electrokinetic Separation and Detection of DNA Nanoparticles in High-Conductance Solutions. *Electrophoresis* 2008, 29, 1765–1774. [PubMed: 18393345]
- (102). Kalyanasundaram D; Inoue S; Kim J-H; Lee H-B; Kawabata Z; Yeo W-H; Cangelosi GA; Oh K; Gao D; Lee K-H; Chung J-H Electric Field-Induced Concentration and Capture of DNA onto Microtips. *Microfluid. Nanofluid* 2012, 13, 217–225.
- (103). Kim D; Shim J; Chuang H-S; Kim KC Effect of Array and Shape of Insulating Posts on Proteins Focusing by Direct Current Dielectrophoresis. *Journal of Mechanical Science and Technology* 2014, 28, 2629–2636.
- (104). Yeo WH; Kopacz AM; Kim JH; Chen X; Wu J; Gao D; Lee KH; Liu WK; Chung JH Dielectrophoretic Concentration of Low-Abundance Nanoparticles Using a Nanostructured Tip. *Nanotechnology* 2012, 23, 485707. [PubMed: 23137928]
- (105). Liu W; Wang C; Ding H; Shao J; Ding Y AC Electric Field Induced Dielectrophoretic Assembly Behavior of Gold Nanoparticles in a Wide Frequency Range. *Appl. Surf. Sci* 2016, 370, 184–192.
- (106). Durr M; Kentsch J; Muller T; Schnelle T; Stelzle M Microdevices for Manipulation and Accumulation of Micro- and Nanoparticles by Dielectrophoresis. *Electrophoresis* 2003, 24, 722–731. [PubMed: 12601744]
- (107). Cheng IF; Chen TY; Lu RJ; Wu HW Rapid Identification of Bacteria Utilizing Amplified Dielectrophoretic Force-Assisted Nanoparticle-Induced Surface-Enhanced Raman Spectroscopy. *Nanoscale Res. Lett* 2014, 9, 324. [PubMed: 25024685]
- (108). Han CH; Woo SY; Bhardwaj J; Sharma A; Jang J Rapid and Selective Concentration of Bacteria, Viruses, and Proteins Using Alternating Current Signal Superimposition on Two Coplanar Electrodes. *Sci. Rep* 2018, 8, 14942. [PubMed: 30297764]
- (109). Yeo WH; Lee HB; Kim JH; Lee KH; Chung JH Nanotip Analysis for Dielectrophoretic Concentration of Nanosized Viral Particles. *Nanotechnology* 2013, 24, 185502. [PubMed: 23579415]
- (110). Zhu J; Xuan X Particle Electrophoresis and Dielectrophoresis in Curved Microchannels. *J. Colloid Interface Sci* 2009, 340, 285–290. [PubMed: 19782995]
- (111). Zhang H; Chang H; Neuzil P DEP-on-a-Chip: Dielectrophoresis Applied to Microfluidic Platforms. *Micromachines* 2019, 10, 423.
- (112). Cetin B; Li D Effect of Joule Heating on Electrokinetic Transport. *Electrophoresis* 2008, 29, 994–1005. [PubMed: 18271065]

- (113). Noblitt SD; Kraly JR; VanBuren JM; Hering SV; Collett JL Jr.; Henry CS Integrated Membrane Filters for Minimizing Hydrodynamic Flow and Filtering in Microfluidic Devices. *Anal. Chem* 2007, 79, 6249–6254. [PubMed: 17636868]
- (114). Striemer CC; Gaborski TR; McGrath JL; Fauchet PM Charge- and Size-Based Separation of Macromolecules Using Ultrathin Silicon Membranes. *Nature* 2007, 445, 749–753. [PubMed: 17301789]
- (115). Fan X; Jia C; Yang J; Li G; Mao H; Jin Q; Zhao J A Microfluidic Chip Integrated with a High-Density PDMS-Based Microfiltration Membrane for Rapid Isolation and Detection of Circulating Tumor Cells. *Biosens. Bioelectron* 2015, 71, 380–386. [PubMed: 25950932]
- (116). Wei H; Chueh BH; Wu H; Hall EW; Li CW; Schirhagl R; Lin JM; Zare RN Particle Sorting Using a Porous Membrane in a Microfluidic Device. *Lab Chip* 2011, 11, 238–245. [PubMed: 21057685]
- (117). Pamme N Continuous Flow Separations in Microfluidic Devices. *Lab Chip* 2007, 7, 1644–1659. [PubMed: 18030382]
- (118). Giddings JC Field-Flow Fractionation: Analysis of Macromolecular, Colloidal, and Particulate Materials. *Science* 1993, 260, 1456–1465. [PubMed: 8502990]
- (119). Vernhet A; Dubascoux S; Cabane B; Fulcrand H; Dubreucq E; Poncet-Legrand C Characterization of Oxidized Tannins: Comparison of Depolymerization Methods, Asymmetric Flow Field-Flow Fractionation and Small-Angle X-Ray Scattering. *Anal. Bioanal. Chem* 2011, 401, 1559–1569. [PubMed: 21573842]
- (120). Loeschner K; Navratilova J; Legros S; Wagner S; Grombe R; Snell J; von der Kammer F; Larsen EH Optimization and Evaluation of Asymmetric Flow Field-Flow Fractionation of Silver Nanoparticles. *J. Chromatogr A* 2013, 1272, 116–125. [PubMed: 23261297]
- (121). Loeschner K; Navratilova J; Købler C; Mølhav K; Wagner S; von der Kammer F; Larsen EH Detection and Characterization of Silver Nanoparticles in Chicken Meat by Asymmetric Flow Field Flow Fractionation with Detection by Conventional or Single Particle ICP-MS. *Anal. Bioanal. Chem* 2013, 405, 8185–8195. [PubMed: 23887279]
- (122). Kammer FVD; Legros S; Hofmann T; Larsen EH; Loeschner K Separation and Characterization of Nanoparticles in Complex Food and Environmental Samples by Field-Flow Fractionation. *TrAC, Trends Anal. Chem* 2011, 30, 425–436.
- (123). Zhang H; Freitas D; Kim HS; Fabijanic K; Li Z; Chen H; Mark MT; Molina H; Martin AB; Bojmar L; Fang J; Rampersaud S; Hoshino A; Matei I; Kenific CM; Nakajima M; Mutvei AP; Sansone P; Buehring W; Wang H; et al. Identification of Distinct Nanoparticles and Subsets of Extracellular Vesicles by Asymmetric Flow Field-Flow Fractionation. *Nat. Cell Biol* 2018, 20, 332–343. [PubMed: 29459780]
- (124). Davies RT; Kim J; Jang SC; Choi EJ; Gho YS; Park J Microfluidic Filtration System to Isolate Extracellular Vesicles from Blood. *Lab Chip* 2012, 12, 5202–5210. [PubMed: 23111789]
- (125). Liang LG; Kong MQ; Zhou S; Sheng YF; Wang P; Yu T; Inci F; Kuo WP; Li LJ; Demirci U; Wang S An Integrated Double-Filtration Microfluidic Device for Isolation, Enrichment and Quantification of Urinary Extracellular Vesicles for Detection of Bladder Cancer. *Sci. Rep* 2017, 7, 46224. [PubMed: 28436447]
- (126). Ang KM; Yeo LY; Hung YM; Tan MK Acoustically-Mediated Microfluidic Nanofiltration through Graphene Films. *Nanoscale* 2017, 9, 6497–6508. [PubMed: 28466906]
- (127). Haefner S; Frank P; Langer E; Gruner D; Schmidt U; Elstner M; Gerlach G; Richter A Chemically Controlled Micro-Pores and Nano-Filters for Separation Tasks in 2D and 3D Microfluidic Systems. *RSC Adv.* 2017, 7, 49279–49289.
- (128). McGrath J; Jimenez M; Bridle H Deterministic Lateral Displacement for Particle Separation: A Review. *Lab Chip* 2014, 14, 4139–4158. [PubMed: 25212386]
- (129). Salafi T; Zhang Y; Zhang Y A Review on Deterministic Lateral Displacement for Particle Separation and Detection. *Nano-Micro Lett.* 2019, 11, 77.
- (130). Huang LR; Cox EC; Austin RH; Sturm JC Continuous Particle Separation through Deterministic Lateral Displacement. *Science* 2004, 304, 987–990. [PubMed: 15143275]



- (131). Santana SM; Antonyak MA; Cerione RA; Kirby BJ Microfluidic Isolation of Cancer-Cell-Derived Microvesicles from Heterogeneous Extracellular Shed Vesicle Populations. *Biomed. Microdevices* 2014, 16, 869–877. [PubMed: 25342569]
- (132). Wunsch BH; Smith JT; Gifford SM; Wang C; Brink M; Bruce RL; Austin RH; Stolovitzky G; Astier Y Nanoscale Lateral Displacement Arrays for the Separation of Exosomes and Colloids Down to 20 nm. *Nat. Nanotechnol* 2016, 11, 936–940. [PubMed: 27479757]
- (133). Zeming KK; Thakor NV; Zhang Y; Chen CH Real-Time Modulated Nanoparticle Separation with an Ultra-Large Dynamic Range. *Lab Chip* 2016, 16, 75–85. [PubMed: 26575003]
- (134). Chen Y; Abrams ES; Boles TC; Pedersen JN; Flyvbjerg H; Austin RH; Sturm JC Concentrating Genomic Length DNA in a Microfabricated Array. *Phys. Rev. Lett* 2015, 114, 198303. [PubMed: 26024203]
- (135). Amini H; Lee W; Di Carlo D Inertial Microfluidic Physics. *Lab Chip* 2014, 14, 2739–2761. [PubMed: 24914632]
- (136). Di Carlo D; Edd JF; Irimia D; Tompkins RG; Toner M Equilibrium Separation and Filtration of Particles Using Differential Inertial Focusing. *Anal. Chem* 2008, 80, 2204–2211. [PubMed: 18275222]
- (137). Kuntaegowdanahalli SS; Bhagat AA; Kumar G; Papautsky I Inertial Microfluidics for Continuous Particle Separation in Spiral Microchannels. *Lab Chip* 2009, 9, 2973–2980. [PubMed: 19789752]
- (138). Martel JM; Toner M Inertial Focusing in Microfluidics. *Annu. Rev. Biomed. Eng* 2014, 16, 371–396. [PubMed: 24905880]
- (139). Zhang J; Yan S; Yuan D; Alici G; Nguyen NT; Ebrahimi Warkiani M; Li W Fundamentals and Applications of Inertial Microfluidics: A Review. *Lab Chip* 2016, 16, 10–34. [PubMed: 26584257]
- (140). Zhou J; Papautsky I Fundamentals of Inertial Focusing in Microchannels. *Lab Chip* 2013, 13, 1121–1132. [PubMed: 23353899]
- (141). Stoecklein D; Di Carlo D Nonlinear Microfluidics. *Anal. Chem* 2019, 91, 296–314. [PubMed: 30501182]
- (142). Bhagat AAS; Kuntaegowdanahalli SS; Papautsky I Inertial Microfluidics for Continuous Particle Filtration and Extraction. *Microfluid. Nanofluid* 2009, 7, 217–226.
- (143). Liu C; Ding B; Xue C; Tian Y; Hu G; Sun J Sheathless Focusing and Separation of Diverse Nanoparticles in Viscoelastic Solutions with Minimized Shear Thinning. *Anal. Chem* 2016, 88, 12547–12553. [PubMed: 28193038]
- (144). Liu C; Guo J; Tian F; Yang N; Yan F; Ding Y; Wei J; Hu G; Nie G; Sun J Field-Free Isolation of Exosomes from Extracellular Vesicles by Microfluidic Viscoelastic Flows. *ACS Nano* 2017, 11, 6968–6976. [PubMed: 28679045]
- (145). Wang L; Dandy DS High-Throughput Inertial Focusing of Micrometer- and Sub-Micrometer-Sized Particles Separation. *Adv. Sci. (Weinh)* 2017, 4, 1700153. [PubMed: 29051857]
- (146). Young Kim J; Won Ahn S; Sik Lee S; Min Kim J Lateral Migration and Focusing of Colloidal Particles and DNA Molecules under Viscoelastic Flow. *Lab Chip* 2012, 12, 2807–2814. [PubMed: 22776909]
- (147). Zhou Y; Ma Z; Tayebi M; Ai Y Submicron Particle Focusing and Exosome Sorting by Wavy Microchannel Structures within Viscoelastic Fluids. *Anal. Chem* 2019, 91, 4577–4584. [PubMed: 30832474]
- (148). Godin J; Chen C-H; Cho SH; Qiao W; Tsai F; Lo Y-H Microfluidics and Photonics for Bio-System-on-a-Chip: A Review of Advancements in Technology Towards a Microfluidic Flow Cytometry Chip. *J. Biophotonics* 2008, 1, 355–376. [PubMed: 19343660]
- (149). Erickson D; Sinton D; Psaltis D Optofluidics for Energy Applications. *Nat. Photonics* 2011, 5, 583–590.
- (150). Yang AHJ; Moore SD; Schmidt BS; Klug M; Lipson M; Erickson D Optical Manipulation of Nanoparticles and Biomolecules in Sub-Wavelength Slot Waveguides. *Nature* 2009, 457, 71–75. [PubMed: 19122638]
- (151). Fan X; White IM Optofluidic Microsystems for Chemical and Biological Analysis. *Nat. Photonics* 2011, 5, 591–597. [PubMed: 22059090]



- (152). Monat C; Domachuk P; Eggleton B Integrated Optofluidics: A New River of Light. *Nat. Photonics* 2007, 1, 106–114.
- (153). Psaltis D; Quake SR; Yang C Developing Optofluidic Technology through the Fusion of Microfluidics and Optics. *Nature* 2006, 442, 381–386. [PubMed: 16871205]
- (154). Shi YZ; Xiong S; Chin LK; Yang Y; Zhang JB; Ser W; Wu JH; Chen TN; Yang ZC; Hao YL; Liedberg B; Yap PH; Zhang Y; Liu AQ High-Resolution and Multi-Range Particle Separation by Microscopic Vibration in an Optofluidic Chip. *Lab Chip* 2017, 17, 2443–2450. [PubMed: 28634603]
- (155). Cuhe A; Canaguier-Durand A; Devaux E; Hutchison JA; Genet C; Ebbesen TW Sorting Nanoparticles with Intertwined Plasmonic and Thermo-Hydrodynamical Forces. *Nano Lett.* 2013, 13, 4230–4235. [PubMed: 23927628]
- (156). Ploschner M; Cizmar T; Mazilu M; Di Falco A; Dholakia K Bidirectional Optical Sorting of Gold Nanoparticles. *Nano Lett.* 2012, 12, 1923–1927. [PubMed: 22448854]
- (157). Shi Y; Zhao H; Chin LK; Zhang Y; Yap PH; Ser W; Qiu CW; Liu AQ Optical Potential-Well Array for High-Selectivity, Massive Trapping and Sorting at Nanoscale. *Nano Lett.* 2020, 20, 5193–5200. [PubMed: 32574502]
- (158). Shi Y; Zhu T; Zhang T; Mazzulla A; Tsai DP; Ding W; Liu AQ; Cipparrone G; Sáenz JJ; Qiu C-W Chirality-Assisted Lateral Momentum Transfer for Bidirectional Enantioselective Separation. *Light: Sci. Appl* 2020, 9, 62. [PubMed: 32337026]
- (159). Zhu T; Shi Y; Ding W; Tsai DP; Cao T; Liu AQ; Nieto-Vesperinas M; Sáenz JJ; Wu PC; Qiu C-W Extraordinary Multipole Modes and Ultra-Enhanced Optical Lateral Force by Chirality. *Phys. Rev. Lett* 2020, 125, No. 043901. [PubMed: 32794795]
- (160). Shi YZ; Xiong S; Zhang Y; Chin LK; Chen YY; Zhang JB; Zhang TH; Ser W; Larsson A; Lim SH; Wu JH; Chen TN; Yang ZC; Hao YL; Liedberg B; Yap PH; Wang K; Tsai DP; Qiu CW; Liu AQ Sculpting Nanoparticle Dynamics for Single-Bacteria-Level Screening and Direct Binding-Efficiency Measurement. *Nat. Commun* 2018, 9, 815. [PubMed: 29483548]
- (161). Shi Y; Zhao H; Nguyen KT; Zhang Y; Chin LK; Zhu T; Yu Y; Cai H; Yap PH; Liu PY; Xiong S; Zhang J; Qiu C-W; Chan CT; Liu AQ Nanophotonic Array-Induced Dynamic Behavior for Label-Free Shape-Selective Bacteria Sieving. *ACS Nano* 2019, 13, 12070–12080. [PubMed: 31585042]
- (162). Nan F; Yan Z Sorting Metal Nanoparticles with Dynamic and Tunable Optical Driven Forces. *Nano Lett.* 2018, 18, 4500–4505. [PubMed: 29939760]
- (163). Shilkin DA; Lyubin EV; Shcherbakov MR; Lapine M; Fedyanin AA Directional Optical Sorting of Silicon Nanoparticles. *ACS Photonics* 2017, 4, 2312–2319.
- (164). Wu W; Zhu X; Zuo Y; Liang L; Zhang S; Zhang X; Yang Y Precise Sorting of Gold Nanoparticles in a Flowing System. *ACS Photonics* 2016, 3, 2497–2504.
- (165). Shi Y; Xiong S; Chin LK; Zhang J; Ser W; Wu J; Chen T; Yang Z; Hao Y; Liedberg B; Yap PH; Tsai DP; Qiu CW; Liu AQ Nanometer-Precision Linear Sorting with Synchronized Optofluidic Dual Barriers. *Sci. Adv* 2018, 4, eaao0773. [PubMed: 29326979]
- (166). Braun M; Wurger A; Cichos F Trapping of Single Nano-Objects in Dynamic Temperature Fields. *Phys. Chem. Chem. Phys* 2014, 16, 15207–15213. [PubMed: 24939651]
- (167). Peng X; Lin L; Hill EH; Kunal P; Humphrey SM; Zheng Y Optothermophoretic Manipulation of Colloidal Particles in Nonionic Liquids. *J. Phys. Chem. C* 2018, 122, 24226–24234.
- (168). Winterer F; Maier CM; Pernpeintner C; Lohmuller T Optofluidic Transport and Manipulation of Plasmonic Nanoparticles by Thermocapillary Convection. *Soft Matter* 2018, 14, 628–634. [PubMed: 29265159]
- (169). Wang B-X; Wang G-Z Plasmonic Nanoparticle Trapping with Inhomogeneous Temperature Fields. *IEEE Photonics J.* 2016, 8, 5502408.
- (170). Weinert FM; Braun D An Optical Conveyor for Molecules. *Nano Lett.* 2009, 9, 4264–4267. [PubMed: 19807065]
- (171). Yu LH; Chen YF Concentration-Dependent Thermophoretic Accumulation for the Detection of DNA Using DNA-Functionalized Nanoparticles. *Anal. Chem* 2015, 87, 2845–2851. [PubMed: 25646686]

- (172). Donner JS; Baffou G; McCloskey D; Quidant R Plasmon-Assisted Optofluidics. *ACS Nano* 2011, 5, 5457–5462. [PubMed: 21657203]
- (173). Baffou G; Quidant R Thermo-Plasmonics: Using Metallic Nanostructures as Nano-Sources of Heat. *Laser & Photonics Reviews* 2013, 7, 171–187.
- (174). Li J; Zhao F; Deng Y; Liu D; Chen CH; Shih WC Photothermal Generation of Programmable Microbubble Array on Nanoporous Gold Disks. *Opt. Express* 2018, 26, 16893–16902. [PubMed: 30119508]
- (175). Braun M; Cichos F Optically Controlled Thermophoretic Trapping of Single Nano-Objects. *ACS Nano* 2013, 7, 11200–11208. [PubMed: 24215133]
- (176). Kirby BJ; Hasselbrink EF Jr. Zeta Potential of Microfluidic Substrates: 1. Theory, Experimental Techniques, and Effects on Separations. *Electrophoresis* 2004, 25, 187–202. [PubMed: 14743473]
- (177). Li D *Electrokinetics in Microfluidics*; Elsevier: Amsterdam, 2004.
- (178). Novo P; Janasek D Current Advances and Challenges in Microfluidic Free-Flow Electrophoresis—a Critical Review. *Anal. Chim. Acta* 2017, 991, 9–29. [PubMed: 29031303]
- (179). Ou X; Chen P; Huang X; Li S; Liu BF Microfluidic Chip Electrophoresis for Biochemical Analysis. *J. Sep. Sci* 2020, 43, 258–270. [PubMed: 31654552]
- (180). Wu D; Qin J; Lin B Electrophoretic Separations on Microfluidic Chips. *J. Chromatogr A* 2008, 1184, 542–559. [PubMed: 18207148]
- (181). Johansson BG Agarose Gel Electrophoresis. *Scand. J. Clin. Lab. Invest* 1972, 29, 7–19.
- (182). Unlu M; Morgan ME; Minden JS Difference Gel Electrophoresis: A Single Gel Method for Detecting Changes in Protein Extracts. *Electrophoresis* 1997, 18, 2071–2077. [PubMed: 9420172]
- (183). Reed C *Capillary Electrophoresis (CE): Principles, Challenges and Applications*; Nova Publisher: New York, 2015.
- (184). Allen RC; Budowle B *Gel Electrophoresis of Proteins and Nucleic Acids: Selected Techniques*; W. de Gruyter: Berlin, 1994.
- (185). Long Z; Liu D; Ye N; Qin J; Lin B Integration of Nanoporous Membranes for Sample Filtration/Preconcentration in Microchip Electrophoresis. *Electrophoresis* 2006, 27, 4927–4934. [PubMed: 17117457]
- (186). Sun W-W; Dai R-J; Li Y-R; Dai G-X; Liu X-J; Li B; Lv X.-f.; Deng Y-L; Luo A-Q Separation of Proteins and DNA by Microstructure-Changed Microfluidic Free Flow Electrophoresis Chips. *Acta Astronaut.* 2020, 166, 573.
- (187). Jeon H; Kim Y; Lim G Continuous Particle Separation Using Pressure-Driven Flow-Induced Miniaturizing Free-Flow Electrophoresis (PDF-Induced MU-FFE). *Sci. Rep* 2016, 6, 19911. [PubMed: 26819221]
- (188). Hanauer M; Pierrat S; Zins I; Lotz A; Sonnichsen C Separation of Nanoparticles by Gel Electrophoresis According to Size and Shape. *Nano Lett.* 2007, 7, 2881–2885. [PubMed: 17718532]
- (189). Kang KH; Kang Y; Xuan X; Li D Continuous Separation of Microparticles by Size with Direct Current-Dielectrophoresis. *Electrophoresis* 2006, 27, 694–702. [PubMed: 16385598]
- (190). Kohlheyer D; Eijkel JC; Schlautmann S; van den Berg A; Schasfoort RB Microfluidic High-Resolution Free-Flow Isoelectric Focusing. *Anal. Chem* 2007, 79, 8190–8198. [PubMed: 17902700]
- (191). Wen J; Wilker EW; Yaffe MB; Jensen KF Microfluidic Preparative Free-Flow Isoelectric Focusing: System Optimization for Protein Complex Separation. *Anal. Chem* 2010, 82, 1253–1260. [PubMed: 20092256]
- (192). Storm G; Belliot SO; Daemen T; Lasic DD Surface Modification of Nanoparticles to Oppose Uptake by the Mononuclear Phagocyte System. *Adv. Drug Delivery Rev* 1995, 17, 31–48.
- (193). Kango S; Kalia S; Celli A; Njuguna J; Habibi Y; Kumar R Surface Modification of Inorganic Nanoparticles for Development of Organic-Inorganic Nanocomposites—a Review. *Prog. Polym. Sci* 2013, 38, 1232–1261.

- (194). Sperling RA; Parak WJ Surface Modification, Functionalization and Bioconjugation of Colloidal Inorganic Nanoparticles. *Philos. Trans. R. Soc., A* 2010, 368, 1333–1383.
- (195). Wang J; Xia J Capillary Electrophoretic Studies on Displacement and Proteolytic Cleavage of Surface Bound Oligohistidine Peptide on Quantum Dots. *Anal. Chim. Acta* 2012, 709, 120–127. [PubMed: 22122940]
- (196). Kohlheyer D; Eijkel JC; Schlautmann S; van den Berg A; Schasfoort RB Bubble-Free Operation of a Microfluidic Free-Flow Electrophoresis Chip with Integrated Pt Electrodes. *Anal. Chem* 2008, 80, 4111–4118. [PubMed: 18435546]
- (197). Frost NW; Bowser MT Using Buffer Additives to Improve Analyte Stream Stability in Micro Free Flow Electrophoresis. *Lab Chip* 2010, 10, 1231–1236. [PubMed: 20445874]
- (198). Becker M; Marggraf U; Janasek D Separation of Proteins Using a Novel Two-Depth Miniaturized Free-Flow Electrophoresis Device with Multiple Outlet Fractionation Channels. *J. Chromatogr A* 2009, 1216, 8265–8269. [PubMed: 19631324]
- (199). Chen C; Skog J; Hsu CH; Lessard RT; Balaj L; Wurdinger T; Carter BS; Breakefield XO; Toner M; Irimia D Microfluidic Isolation and Transcriptome Analysis of Serum Microvesicles. *Lab Chip* 2010, 10, 505–511. [PubMed: 20126692]
- (200). Kanwar SS; Dunlay CJ; Simeone DM; Nagraath S Microfluidic Device (Exochip) for on-Chip Isolation, Quantification and Characterization of Circulating Exosomes. *Lab Chip* 2014, 14, 1891–1900. [PubMed: 24722878]
- (201). Lo TW; Zhu Z; Purcell E; Watzka D; Wang J; Kang YT; Jolly S; Nagraath D; Nagraath S Microfluidic Device for High-Throughput Affinity-Based Isolation of Extracellular Vesicles. *Lab Chip* 2020, 20, 1762–1770. [PubMed: 32338266]
- (202). Zhang P; He M; Zeng Y Ultrasensitive Microfluidic Analysis of Circulating Exosomes Using a Nanostructured Graphene Oxide/Polydopamine Coating. *Lab Chip* 2016, 16, 3033–3042. [PubMed: 27045543]
- (203). Reategui E; van der Vos KE; Lai CP; Zeinali M; Atai NA; Aldikacti B; Floyd FP Jr.; A HK; Thapar V; Hochberg FH; Sequist LV; Nahed BV; B SC; Toner M; Balaj L; D TT; Breakefield XO; Stott SL Engineered Nanointerfaces for Microfluidic Isolation and Molecular Profiling of Tumor-Specific Extracellular Vesicles. *Nat. Commun* 2018, 9, 175. [PubMed: 29330365]
- (204). Zhang P; Zhou X; He M; Shang Y; Tetlow AL; Godwin AK; Zeng Y Ultrasensitive Detection of Circulating Exosomes with a 3D-Nanopatterned Microfluidic Chip. *Nat. Biomed Eng* 2019, 3, 438–451. [PubMed: 31123323]
- (205). He M; Crow J; Roth M; Zeng Y; Godwin AK Integrated Immunoisolation and Protein Analysis of Circulating Exosomes Using Microfluidic Technology. *Lab Chip* 2014, 14, 3773–3780. [PubMed: 25099143]
- (206). Im H; Shao H; Park YI; Peterson VM; Castro CM; Weissleder R; Lee H Label-Free Detection and Molecular Profiling of Exosomes with a Nano-Plasmonic Sensor. *Nat. Biotechnol* 2014, 32, 490–495. [PubMed: 24752081]
- (207). Jeong S; Park J; Pathania D; Castro CM; Weissleder R; Lee H Integrated Magneto-Electrochemical Sensor for Exosome Analysis. *ACS Nano* 2016, 10, 1802–1809. [PubMed: 26808216]
- (208). Wang S; Esfahani M; Gurkan UA; Inci F; Kuritzkes DR; Demirci U Efficient on-Chip Isolation of HIV Subtypes. *Lab Chip* 2012, 12, 1508–1515. [PubMed: 22391989]
- (209). Jackson EA; Hillmyer MA Nanoporous Membranes Derived from Block Copolymers: From Drug Delivery to Water Filtration. *ACS Nano* 2010, 4, 3548–3553. [PubMed: 20695511]
- (210). Shannon MA; Bohn PW; Elimelech M; Georgiadis JG; Marinas BJ; Mayes AM Science and Technology for Water Purification in the Coming Decades. *Nature* 2008, 452, 301–310. [PubMed: 18354474]
- (211). Baker RW Membrane Technology and Applications, 3rd ed.; John Wiley & Sons: Hoboken, NJ, 2012; p 1.
- (212). Cheryan M; Cheryan M Ultrafiltration and Microfiltration Handbook; Technomic Pub. Co.: Lancaster, PA, 1998.
- (213). Yang Z; Zhou Y; Feng Z; Rui X; Zhang T; Zhang Z A Review on Reverse Osmosis and Nanofiltration Membranes for Water Purification. *Polymers (Basel, Switz.)* 2019, 11, 1252.

- (214). Perez-Gonzalez A; Urtiaga AM; Ibanez R; Ortiz I State of the Art and Review on the Treatment Technologies of Water Reverse Osmosis Concentrates. *Water Res.* 2012, 46, 267–283. [PubMed: 22119366]
- (215). Greenlee LF; Lawler DF; Freeman BD; Marrot B; Moulin P Reverse Osmosis Desalination: Water Sources, Technology, and Today's Challenges. *Water Res.* 2009, 43, 2317–2348. [PubMed: 19371922]
- (216). Gaboriski TR; Snyder JL; Striemer CC; Fang DZ; Hoffman M; Fauchet PM; McGrath JL High-Performance Separation of Nanoparticles with Ultrathin Porous Nanocrystalline Silicon Membranes. *ACS Nano* 2010, 4, 6973–6981. [PubMed: 21043434]
- (217). Liang HW; Wang L; Chen PY; Lin HT; Chen LF; He D; Yu SH Carbonaceous Nanofiber Membranes for Selective Filtration and Separation of Nanoparticles. *Adv. Mater* 2010, 22, 4691–4695. [PubMed: 20859940]
- (218). Forster H; Thajudeen T; Funk C; Peukert W Separation of Nanoparticles: Filtration and Scavenging from Waste Incineration Plants. *Waste Manage.* 2016, 52, 346–352.
- (219). Sharma V; Park K; Srinivasarao M Shape Separation of Gold Nanorods Using Centrifugation. *Proc. Natl. Acad. Sci. U. S. A* 2009, 106, 4981–4985. [PubMed: 19255445]
- (220). Arosio P; Muller T; Mahadevan L; Knowles TP Density-Gradient-Free Microfluidic Centrifugation for Analytical and Preparative Separation of Nanoparticles. *Nano Lett.* 2014, 14, 2365–2371. [PubMed: 24611748]
- (221). Akbulut O; Mace CR; Martinez RV; Kumar AA; Nie Z; Patton MR; Whitesides GM Separation of Nanoparticles in Aqueous Multiphase Systems through Centrifugation. *Nano Lett.* 2012, 12, 4060–4064. [PubMed: 22668343]
- (222). Shiddiky MJ; Shim YB Trace Analysis of DNA: Preconcentration, Separation, and Electrochemical Detection in Microchip Electrophoresis Using Au Nanoparticles. *Anal. Chem* 2007, 79, 3724–3733. [PubMed: 17428034]
- (223). Morbioli GG; Mazzu-Nascimento T; Aquino A; Cervantes C; Carrilho E Recombinant Drugs-on-a-Chip: The Usage of Capillary Electrophoresis and Trends in Miniaturized Systems - a Review. *Anal. Chim. Acta* 2016, 935, 44–57. [PubMed: 27543014]
- (224). Molloy MP Two-Dimensional Electrophoresis of Membrane Proteins Using Immobilized pH Gradients. *Anal. Biochem* 2000, 280, 1–10. [PubMed: 10805514]
- (225). Gorg A; Weiss W; Dunn MJ Current Two-Dimensional Electrophoresis Technology for Proteomics. *Proteomics* 2004, 4, 3665–3685. [PubMed: 15543535]
- (226). Boing AN; van der Pol E; Grootemaat AE; Coumans FA; Sturk A; Nieuwland R Single-Step Isolation of Extracellular Vesicles by Size-Exclusion Chromatography. *J. Extracell. Vesicles* 2014, 3, 23430.
- (227). Koh YQ; Almughlliq FB; Vaswani K; Peiris HN; Mitchell MD Exosome Enrichment by Ultracentrifugation and Size Exclusion Chromatography. *Front. Biosci., Landmark Ed* 2018, 23, 865–874. [PubMed: 28930577]
- (228). Pitkanen L; Striegel AM Size-Exclusion Chromatography of Metal Nanoparticles and Quantum Dots. *TrAC, Trends Anal. Chem* 2016, 80, 311–320.
- (229). Welton JL; Webber JP; Botos LA; Jones M; Clayton A Ready-Made Chromatography Columns for Extracellular Vesicle Isolation from Plasma. *J. Extracell. Vesicles* 2015, 4, 27269. [PubMed: 25819214]
- (230). Westermeier R; Gronau S Electrophoresis in Practice: A Guide to Methods and Applications of DNA and Protein Separations, 4th ed. (English); Wiley-VCH: Weinheim, Germany, 2005.
- (231). Mark D; Haeberle S; Roth G; von Stetten F; Zengerle R Microfluidic Lab-on-a-Chip Platforms: Requirements, Characteristics and Applications. *Chem. Soc. Rev* 2010, 39, 1153–1182. [PubMed: 20179830]
- (232). Duffy DC; McDonald JC; Schueller OJ; Whitesides GM Rapid Prototyping of Microfluidic Systems in Poly-(Dimethylsiloxane). *Anal. Chem* 1998, 70, 4974–4984. [PubMed: 21644679]
- (233). Reyes DR; Iossifidis D; Auroux PA; Manz A Micro Total Analysis Systems. 1. Introduction, Theory, and Technology. *Anal. Chem* 2002, 74, 2623–2636. [PubMed: 12090653]
- (234). Thorsen T; Maerkl SJ; Quake SR Microfluidic Large-Scale Integration. *Science* 2002, 298, 580–584. [PubMed: 12351675]

- (235). Salafi T; Zeming KK; Zhang Y Advancements in Microfluidics for Nanoparticle Separation. *Lab Chip* 2017, 17, 11–33.
- (236). Robertson JD; Rizzello L; Avila-Olias M; Gaitzsch J; Contini C; Magon MS; Renshaw SA; Battaglia G Purification of Nanoparticles by Size and Shape. *Sci. Rep* 2016, 6, 27494. [PubMed: 27271538]
- (237). Bhagat AAS; Bow H; Hou HW; Tan SJ; Han J; Lim CT Microfluidics for Cell Separation. *Med. Biol. Eng. Comput* 2010, 48, 999–1014. [PubMed: 20414811]
- (238). Chen J; Li J; Sun Y Microfluidic Approaches for Cancer Cell Detection, Characterization, and Separation. *Lab Chip* 2012, 12, 1753–1767. [PubMed: 22437479]
- (239). Chen Y; Li P; Huang P-H; Xie Y; Mai JD; Wang L; Nguyen N-T; Huang TJ Rare Cell Isolation and Analysis in Microfluidics. *Lab Chip* 2014, 14, 626–645. [PubMed: 24406985]
- (240). Ding X; Peng Z; Lin S-CS; Geri M; Li S; Li P; Chen Y; Dao M; Suresh S; Huang TJ Cell Separation Using Tilted-Angle Standing Surface Acoustic Waves. *Proc. Natl. Acad. Sci. U. S. A* 2014, 111, 12992–12997. [PubMed: 25157150]
- (241). Gossett DR; Weaver WM; Mach AJ; Hur SC; Tse HTK; Lee W; Amini H; Di Carlo D Label-Free Cell Separation and Sorting in Microfluidic Systems. *Anal. Bioanal. Chem* 2010, 397, 3249–3267. [PubMed: 20419490]
- (242). Wyatt Shields C IV; Reyes CD; Lopez GP Microfluidic Cell Sorting: A Review of the Advances in the Separation of Cells from Debulking to Rare Cell Isolation. *Lab Chip* 2015, 15, 1230–1249. [PubMed: 25598308]
- (243). Xie Y; Ahmed D; Lapsley MI; Lu M; Li S; Huang TJ Acoustofluidic Relay: Sequential Trapping and Transporting of Microparticles *via* Acoustically Excited Oscillating Bubbles. *J. Lab Autom* 2014, 19, 137–143. [PubMed: 23592570]
- (244). Jones TB *Electromechanics of Particles*, 1st ed.; Cambridge University Press: New York, 2005.
- (245). Bechinger C; Di Leonardo R; Lowen H; Reichhardt C; Volpe G; Volpe G Active Particles in Complex and Crowded Environments. *Rev. Mod. Phys* 2016, 88, 045006.
- (246). Borodin AN; Salminen P *Handbook of Brownian Motion - Facts and Formulae*; Springer: Berlin, 1996.
- (247). Cui W; Mu L; Duan X; Pang W; Reed MA Trapping of Sub-100 nm Nanoparticles Using Gigahertz Acoustofluidic Tweezers for Biosensing Applications. *Nanoscale* 2019, 11, 14625–14634. [PubMed: 31240289]
- (248). Shilton RJ; Travagliati M; Beltram F; Cecchini M Nanoliter-Droplet Acoustic Streaming *via* Ultra High Frequency Surface Acoustic Waves. *Adv. Mater* 2014, 26, 4941–4946. [PubMed: 24677370]
- (249). Wang YI; Shuler ML Unichip Enables Long-Term Recirculating Unidirectional Perfusion with Gravity-Driven Flow for Microphysiological Systems. *Lab Chip* 2018, 18, 2563–2574. [PubMed: 30046784]
- (250). Garcia-Cordero JL; Basabe-Desmonts L; Ducrée J; Ricco AJ Liquid Recirculation in Microfluidic Channels by the Interplay of Capillary and Centrifugal Forces. *Microfluid. Nanofluid* 2010, 9, 695–703.
- (251). Huh D; Mills KL; Zhu X; Burns MA; Thouless MD; Takayama S Tuneable Elastomeric Nanochannels for Nanofluidic Manipulation. *Nat. Mater* 2007, 6, 424–428. [PubMed: 17486084]
- (252). Stavitskiy SM; Geist J; Gaitan M Separation and Metrology of Nanoparticles by Nanofluidic Size Exclusion. *Lab Chip* 2010, 10, 2618–2621. [PubMed: 20714640]
- (253). Thomas JA; McGaughey AJH Reassessing Fast Water Transport through Carbon Nanotubes. *Nano Lett.* 2008, 8, 2788–2793. [PubMed: 18665654]
- (254). Bocquet L; Charlaix E Nanofluidics, from Bulk to Interfaces. *Chem. Soc. Rev* 2010, 39, 1073–1095. [PubMed: 20179826]
- (255). Taylor R; Coulombe S; Otanicar T; Phelan P; Gunawan A; Lv W; Rosengarten G; Prasher R; Tyagi H Small Particles, Big Impacts: A Review of the Diverse Applications of Nanofluids. *J. Appl. Phys* 2013, 113, 011301.
- (256). Erickson HP Size and Shape of Protein Molecules at the Nanometer Level Determined by Sedimentation, Gel Filtration, and Electron Microscopy. *Biol. Proced. Online* 2009, 11, 32–51. [PubMed: 19495910]



- (257). Zhou L; Yuan J; Yuan W; Sui X; Wu S; Li Z; Shen D Synthesis, Characterization, and Controllable Drug Release of pH-Sensitive Hybrid Magnetic Nanoparticles. *J. Magn. Magn. Mater* 2009, 321, 2799–2804.
- (258). Chithrani BD; Ghazani AA; Chan WC Determining the Size and Shape Dependence of Gold Nanoparticle Uptake into Mammalian Cells. *Nano Lett.* 2006, 6, 662–668. [PubMed: 16608261]
- (259). Pal S; Tak YK; Song JM Does the Antibacterial Activity of Silver Nanoparticles Depend on the Shape of the Nanoparticle? A Study of the Gram-Negative Bacterium *Escherichia Coli*. *Appl. Environ. Microbiol* 2007, 73, 1712–1720. [PubMed: 17261510]
- (260). Turchinovich A; Drapkina O; Tonevitsky A Transcriptome of Extracellular Vesicles: State-of-the-Art. *Front. Immunol* 2019, 10, 202. [PubMed: 30873152]
- (261). Konoshenko MY; Lekchnov EA; Vlassov AV; Laktionov PP Isolation of Extracellular Vesicles: General Methodologies and Latest Trends. *BioMed Res. Int* 2018, 2018, 8545347. [PubMed: 29662902]
- (262). Rosa-Fernandes L; Rocha VB; Carregari VC; Urbani A; Palmisano G A Perspective on Extracellular Vesicles Proteomics. *Front. Chem* 2017, 5, 102. [PubMed: 29209607]
- (263). Shpacovitch V; Hergenroder R Optical and Surface Plasmonic Approaches to Characterize Extracellular Vesicles. *Anal. Chim. Acta* 2018, 1005, 1–15. [PubMed: 29389314]
- (264). Guo SC; Tao SC; Dawn H Microfluidics-Based on-a-Chip Systems for Isolating and Analysing Extracellular Vesicles. *J. Extracell. Vesicles* 2018, 7, 1508271. [PubMed: 30151077]
- (265). Li X; Ballerini DR; Shen W A Perspective on Paper-Based Microfluidics: Current Status and Future Trends. *Biomicrofluidics* 2012, 6, 011301.
- (266). Fu E; Downs C Progress in the Development and Integration of Fluid Flow Control Tools in Paper Microfluidics. *Lab Chip* 2017, 17, 614–628. [PubMed: 28119982]
- (267). Sun H; Chan CW; Wang Y; Yao X; Mu X; Lu X; Zhou J; Cai Z; Ren K Reliable and Reusable Whole Polypropylene Plastic Microfluidic Devices for a Rapid, Low-Cost Antimicrobial Susceptibility Test. *Lab Chip* 2019, 19, 2915–2924. [PubMed: 31369010]
- (268). Boone TD; Fan ZH; Hooper HH; Ricco AJ; Tan H; Williams SJ Plastic Advances Microfluidic Devices. *Anal. Chem* 2002, 74, 78A–86A.
- (269). Aguilera-Gomez A; Rabouille C Membrane-Bound Organelles Versus Membrane-Less Compartments and Their Control of Anabolic Pathways in *Drosophila*. *Dev. Biol* 2017, 428, 310–317. [PubMed: 28377034]
- (270). Jagow GV; Schägger H Membrane Protein Purification and Crystallization: A Practical Guide, 2nd ed.; Academic Press: Boston, 2003.
- (271). Ryan VH; Fawzi NL Physiological, Pathological, and Targetable Membraneless Organelles in Neurons. *Trends Neurosci.* 2019, 42, 693–708. [PubMed: 31493925]
- (272). Brangwynne CP Phase Transitions and Size Scaling of Membrane-Less Organelles. *J. Cell Biol* 2013, 203, 875–881. [PubMed: 24368804]
- (273). Elbaum-Garfinkle S Matter over Mind: Liquid Phase Separation and Neurodegeneration. *J. Biol. Chem* 2019, 294, 7160–7168. [PubMed: 30914480]
- (274). Patel A; Lee HO; Jawerth L; Maharana S; Jahnelt M; Hein MY; Stoykov S; Mahamid J; Saha S; Franzmann TM; Pozniakovski A; Poser I; Maghelli N; Royer LA; Weigert M; Myers EW; Grill S; Drechsel D; Hyman AA; Alberti S A Liquid-to-Solid Phase Transition of the ALS Protein FUS Accelerated by Disease Mutation. *Cell* 2015, 162, 1066–1077. [PubMed: 26317470]
- (275). Molliex A; Temirov J; Lee J; Coughlin M; Kanagaraj AP; Kim HJ; Mittag T; Taylor JP Phase Separation by Low Complexity Domains Promotes Stress Granule Assembly and Drives Pathological Fibrillization. *Cell* 2015, 163, 123–133. [PubMed: 26406374]
- (276). Wolozin B; Ivanov P Stress Granules and Neurodegeneration. *Nat. Rev. Neurosci* 2019, 20, 649–666. [PubMed: 31582840]
- (277). Khong A; Jain S; Matheny T; Wheeler JR; Parker R Isolation of Mammalian Stress Granule Cores for RNA-Seq Analysis. *Methods* 2018, 137, 49–54. [PubMed: 29196162]
- (278). Brigger I; Dubernet C; Couvreur P Nanoparticles in Cancer Therapy and Diagnosis. *Adv. Drug Delivery Rev* 2002, 54, 631–651.



- (279). Blasiak B; van Veggel FCJM; Tomanek B Applications of Nanoparticles for MRI Cancer Diagnosis and Therapy. *J. Nanomater* 2013, 2013, 148578.
- (280). Kanninen KM; Bister N; Koistinaho J; Malm T Exosomes as New Diagnostic Tools in CNS Diseases. *Biochim. Biophys. Acta, Mol. Basis Dis* 2016, 1862, 403–410.
- (281). Qiu Y; Liu Y; Wang L; Xu L; Bai R; Ji Y; Wu X; Zhao Y; Li Y; Chen C Surface Chemistry and Aspect Ratio Mediated Cellular Uptake of Au Nanorods. *Biomaterials* 2010, 31, 7606–7619. [PubMed: 20656344]
- (282). Hung LH; Choi KM; Tseng WY; Tan YC; Shea KJ; Lee AP Alternating Droplet Generation and Controlled Dynamic Droplet Fusion in Microfluidic Device for Cds Nanoparticle Synthesis. *Lab Chip* 2006, 6, 174–178. [PubMed: 16450024]
- (283). Yang CG; Xu ZR; Lee AP; Wang JH A Microfluidic Concentration-Gradient Droplet Array Generator for the Production of Multi-Color Nanoparticles. *Lab Chip* 2013, 13, 2815–2820. [PubMed: 23674199]
- (284). Wang J; Mao W; Lock LL; Tang J; Sui M; Sun W; Cui H; Xu D; Shen Y The Role of Micelle Size in Tumor Accumulation, Penetration, and Treatment. *ACS Nano* 2015, 9, 7195–7206. [PubMed: 26149286]
- (285). Magdolenova Z; Collins A; Kumar A; Dhawan A; Stone V; Dusinska M Mechanisms of Genotoxicity. A Review of in Vitro and in Vivo Studies with Engineered Nanoparticles. *Nanotoxicology* 2014, 8, 233–278. [PubMed: 23379603]

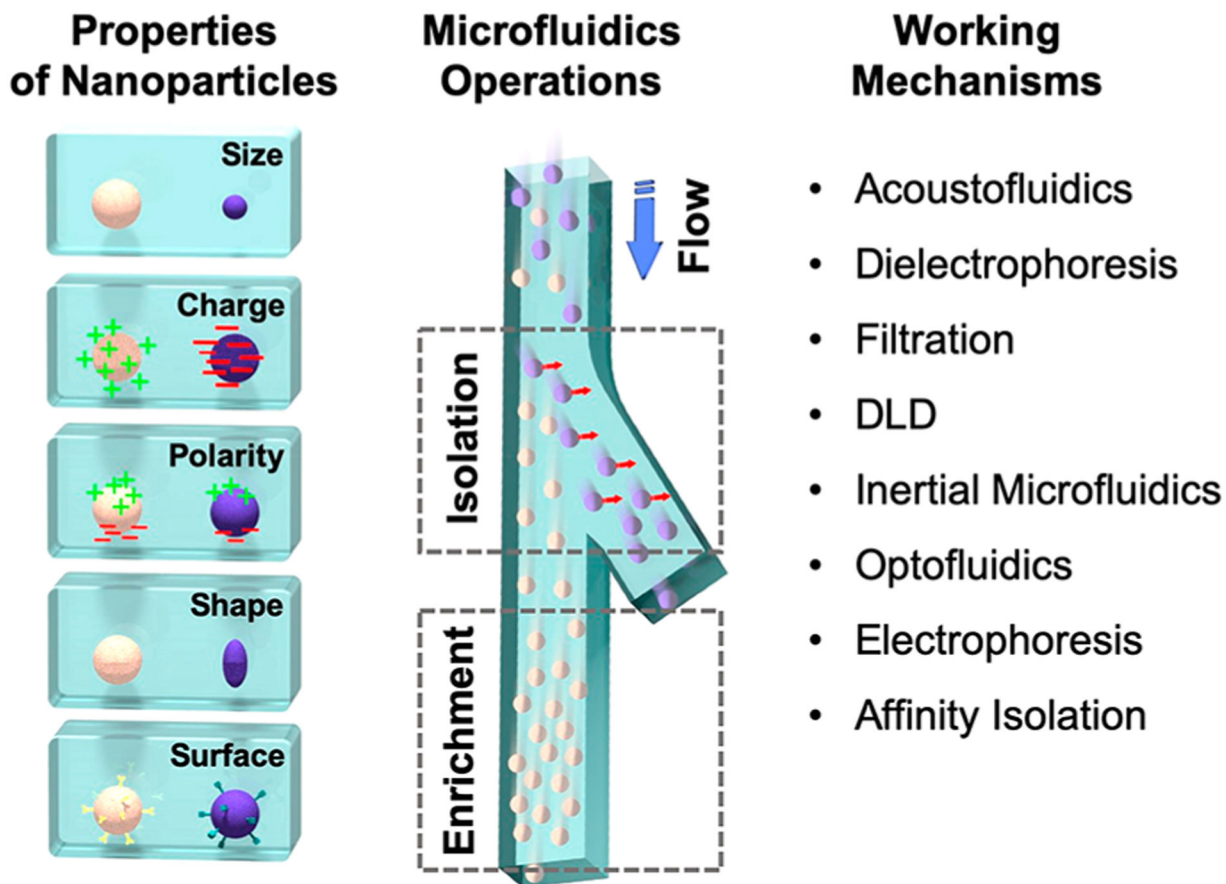


**Figure 1.** Diagram showing the procedures and mechanisms of isolation and enrichment of nanoparticles in a microfluidic system.

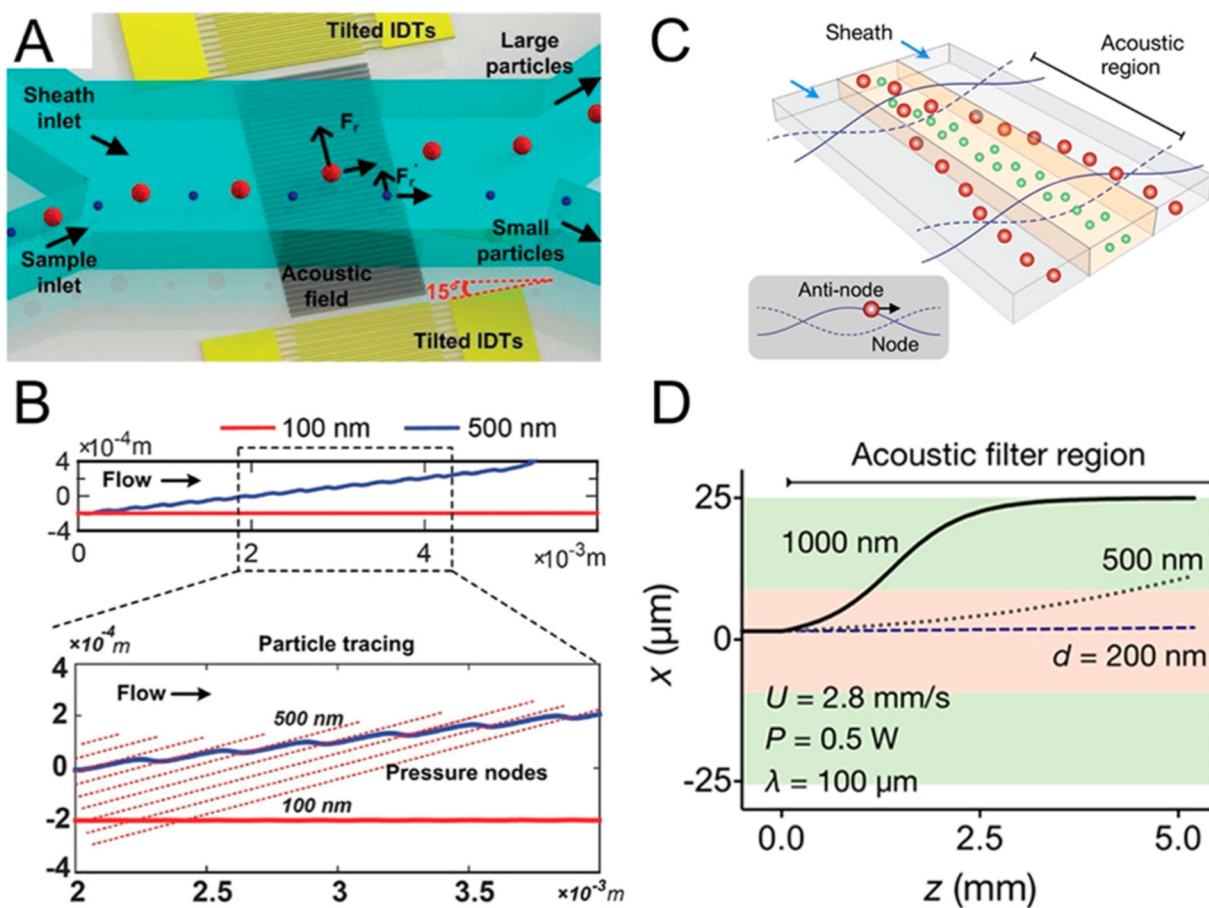


**Figure 2.** Acoustic-enabled nanoparticle separation. (A) Schematic and (B) simulation of the separation of nanoparticles with standing surface acoustic wave fields that are tilted with respect to the microfluidic channel. Reprinted with permission from ref 74. Copyright 2017 Wiley. (C) Schematic and (D) simulation of the separation of nanoparticles using standing surface acoustic wave fields that are parallel to the microfluidic channel. Reprinted from ref 77. Copyright 2015 American Chemical Society.

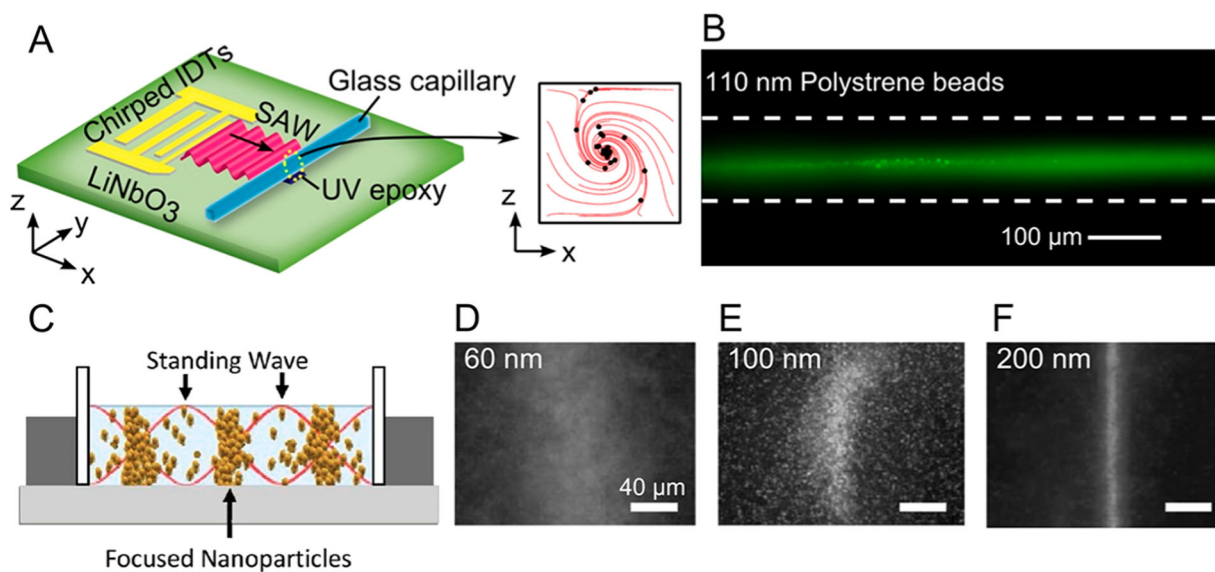


**Figure 3.**

Acoustic enrichment of nanoparticles. (A) Schematic and (B) experimental demonstration of acoustic streaming in a capillary tube that concentrates 110 nm polystyrene beads. Reprinted from ref 43. Copyright 2017 American Chemical Society. (C) Schematic illustrating how the primary acoustic radiation force is used to concentrate nanoparticles at pressure nodes. (D–F) Experimental images showing how the concentration effect is size-dependent. Reprinted with permission from ref 80. Copyright 2018 Wiley.

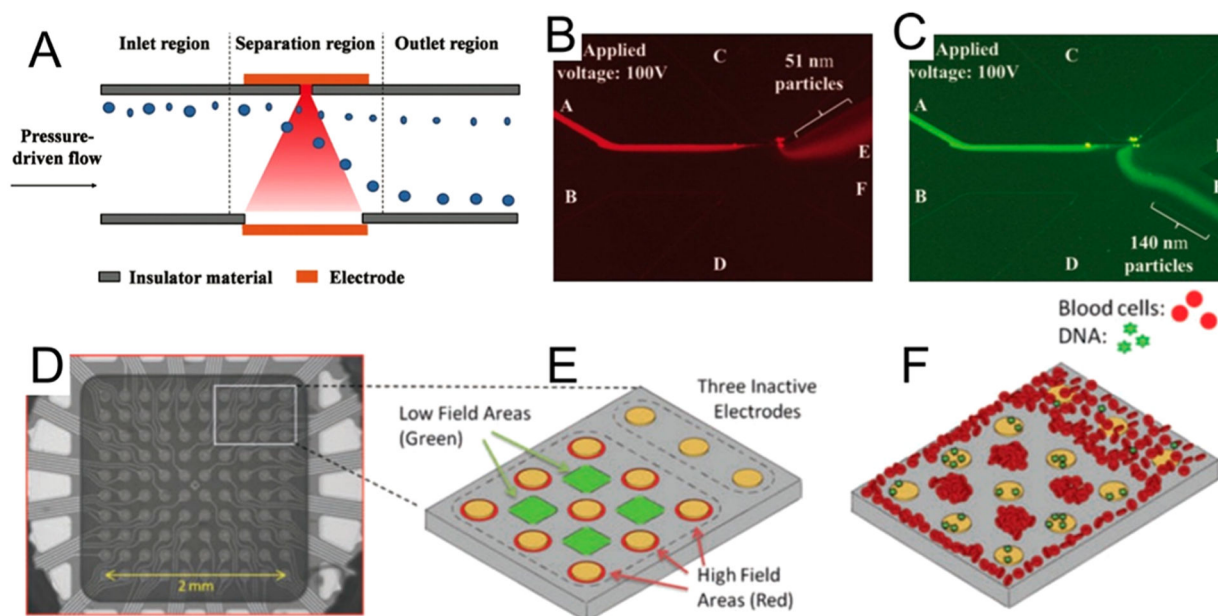


**Figure 4.** Dielectrophoretic-enabled nanoparticle separation. (A) A nano-orifice-based dielectrophoretic method to separate nanoparticles with sizes of (B) 50 and (C) 140 nm. Reprinted with permission from ref 99. Copyright 2016 Royal Society of Chemistry. (D) Microscopic image and (E) schematic of a dielectrophoretic microarray device that works in a semicontinuous manner for (F) separation of DNA and nanoparticles from blood. Reprinted with permission from ref 100. Copyright 2012 Wiley.

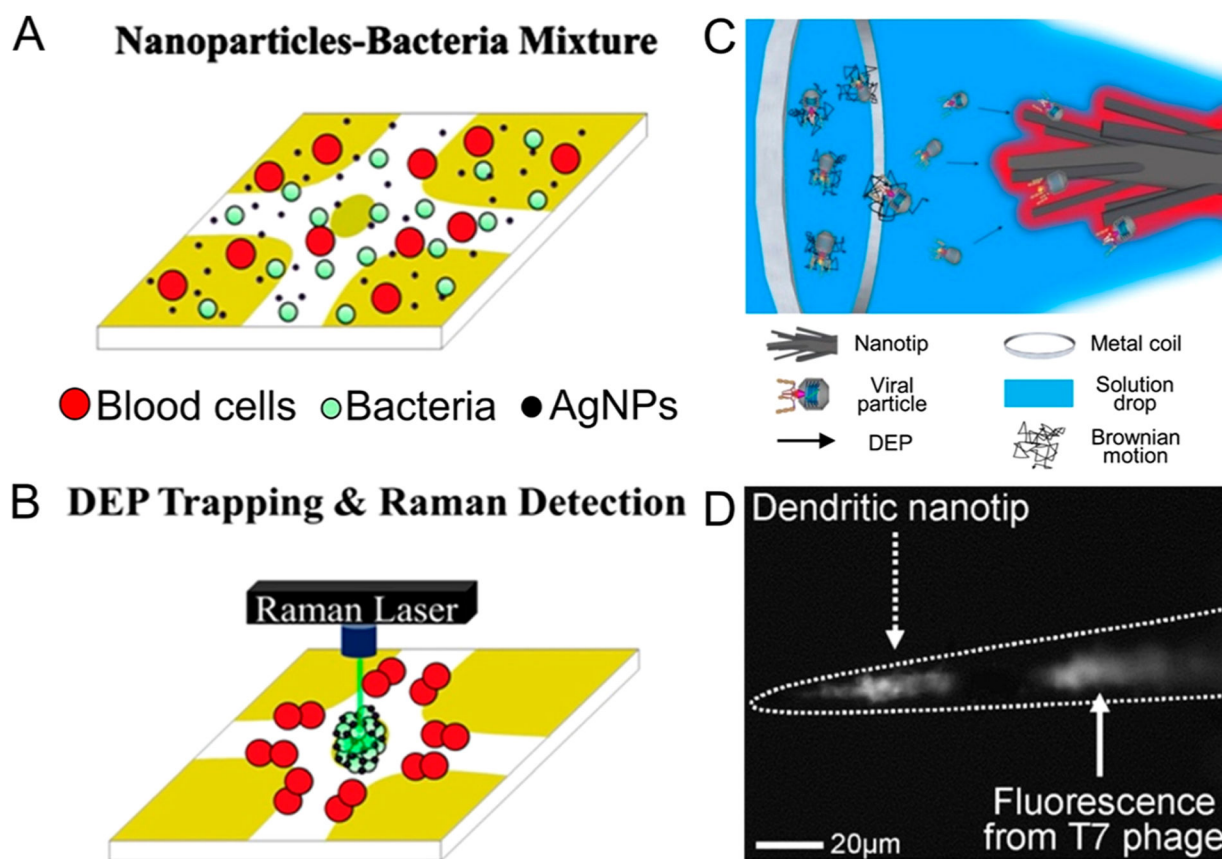


**Figure 5.** Dielectrophoretic (DEP)-enabled nanoparticle enrichment. (A,B) Schematics depicting the DEP concentration of bacteria and Ag nanoparticles with electrodes deposited on a glass substrate. Reprinted with permission from ref 107. Copyright 2014 Springer. (C) Schematic and (D) microscopic image of the DEP concentration of viruses (*i.e.*, T7 phage) on a dendritic nanotip. Reprinted with permission from ref 109. Copyright 2013 IOP Publishing.



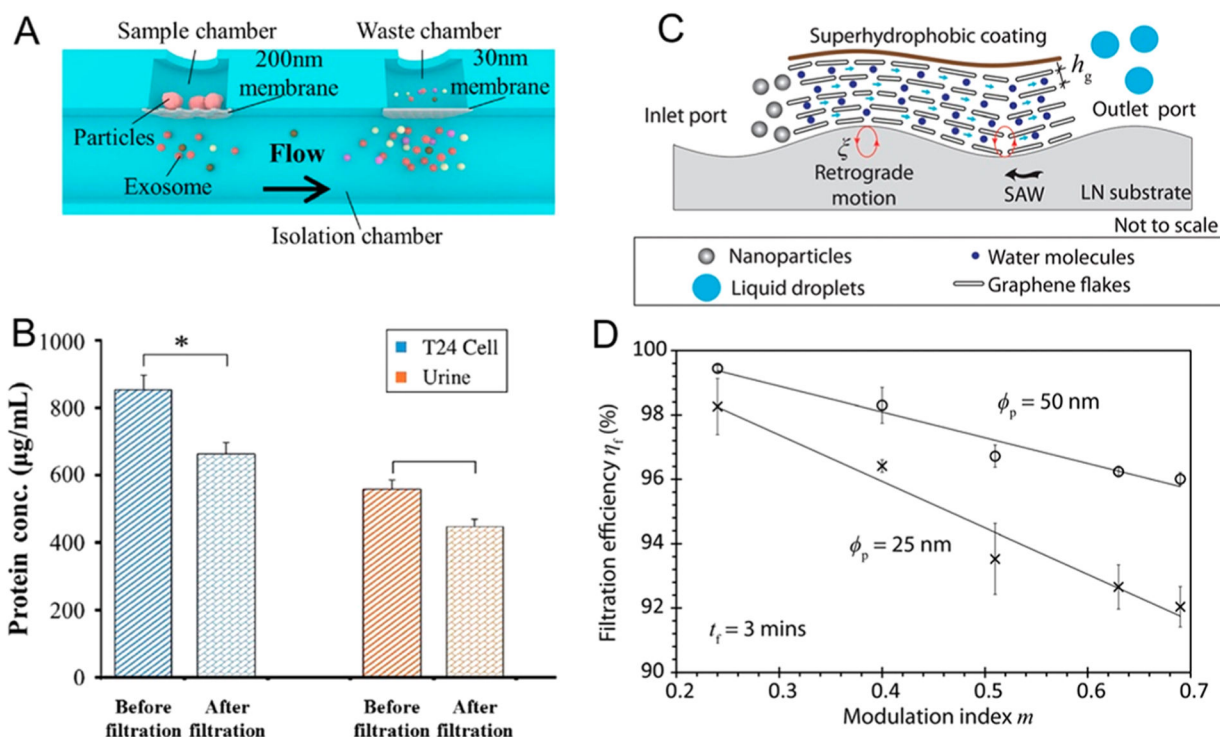


**Figure 6.** Filtration-enabled nanoparticle separation. (A,B) Double-filtration microfluidic device to separate extracellular vesicles from urine and cell cultures. Reprinted with permission from ref 126. Copyright 2017 Royal Society of Chemistry. (C,D) Integrating surface acoustic waves with a graphene filter to isolate nanoparticles suspended in water. Reprinted with permission from ref 125. Copyright 2017 Nature Publishing Group.

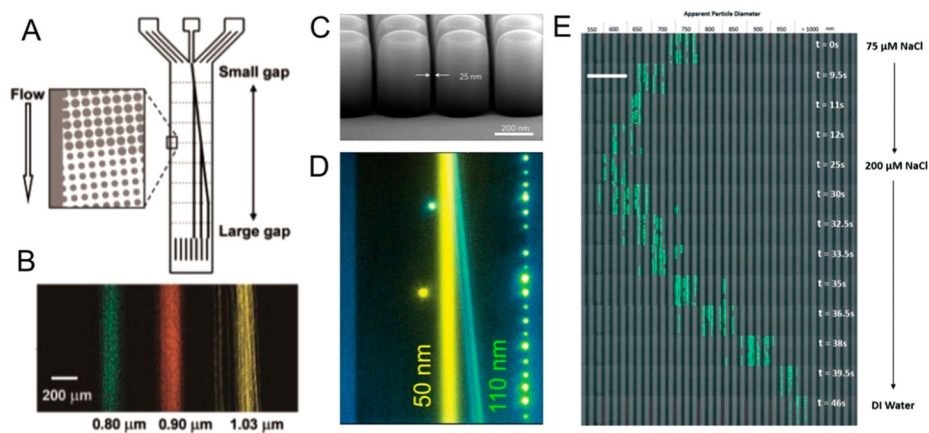


**Figure 7.** DLD-enabled nanoparticle separation. (A,B) DLD separation of nanoparticles with three sizes. Reprinted with permission from ref 130. Copyright 2004 American Association for the Advancement of Science. (C,D) Nano-DLD separates nanoparticles with size differences less than 100 nm. Reprinted with permission from ref 132. Copyright 2016 Nature Publishing Group. (E) Tuning the size of nanoparticles *via* the addition of solvents in DLD separations. Reprinted with permission from ref 133. Copyright 2016 Royal Society of Chemistry.

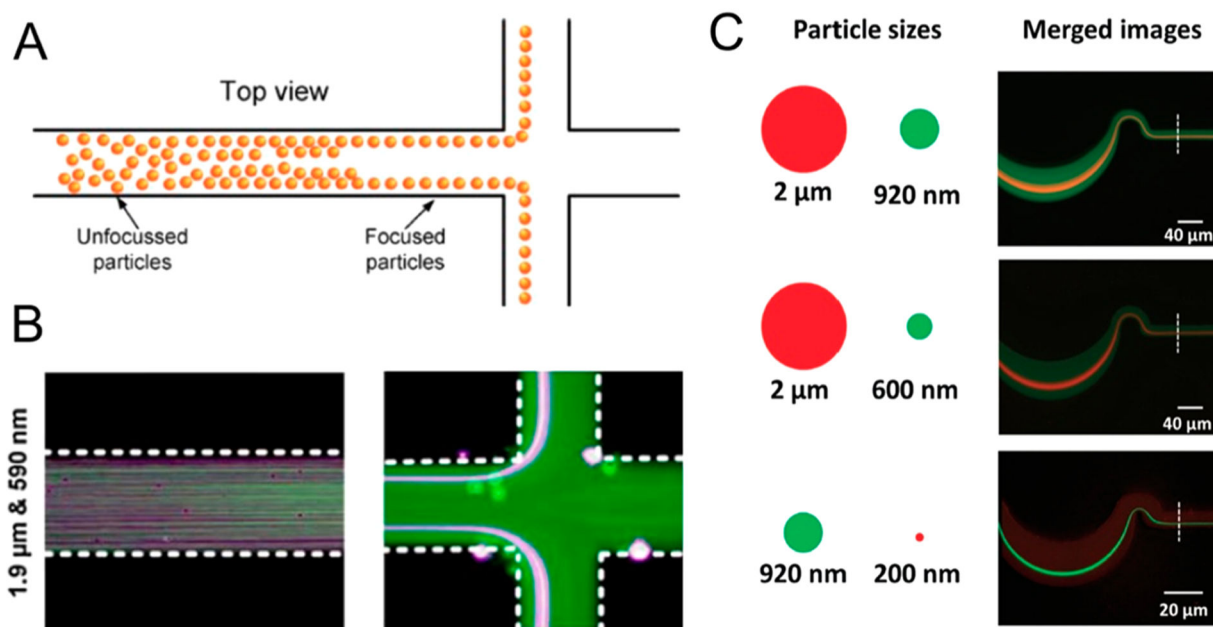


**Figure 8.**

Inertial microfluidic-enabled nanoparticle separation. (A,B) Nanoparticle separation in a straight, rectangular microchannel based on shear-induced inertial lift forces. Reprinted with permission from ref 142. Copyright 2009 Springer. (C) High-throughput nanoparticle separation in a spiral channel. Reprinted with permission from ref 145. Copyright 2017 Wiley.

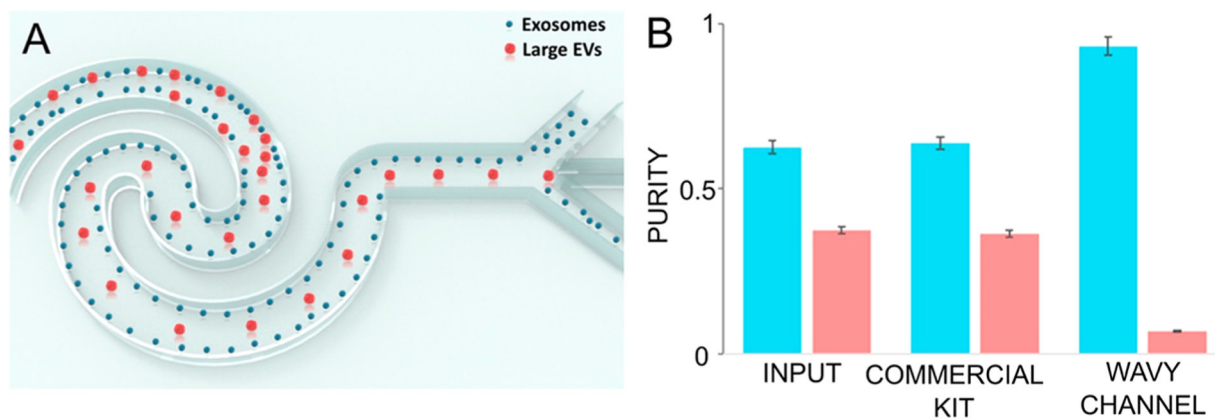


**Figure 9.** Inertial microfluidics-based enrichment and isolation of exosomes. Reprinted from ref 147. Copyright 2019 American Chemical Society.

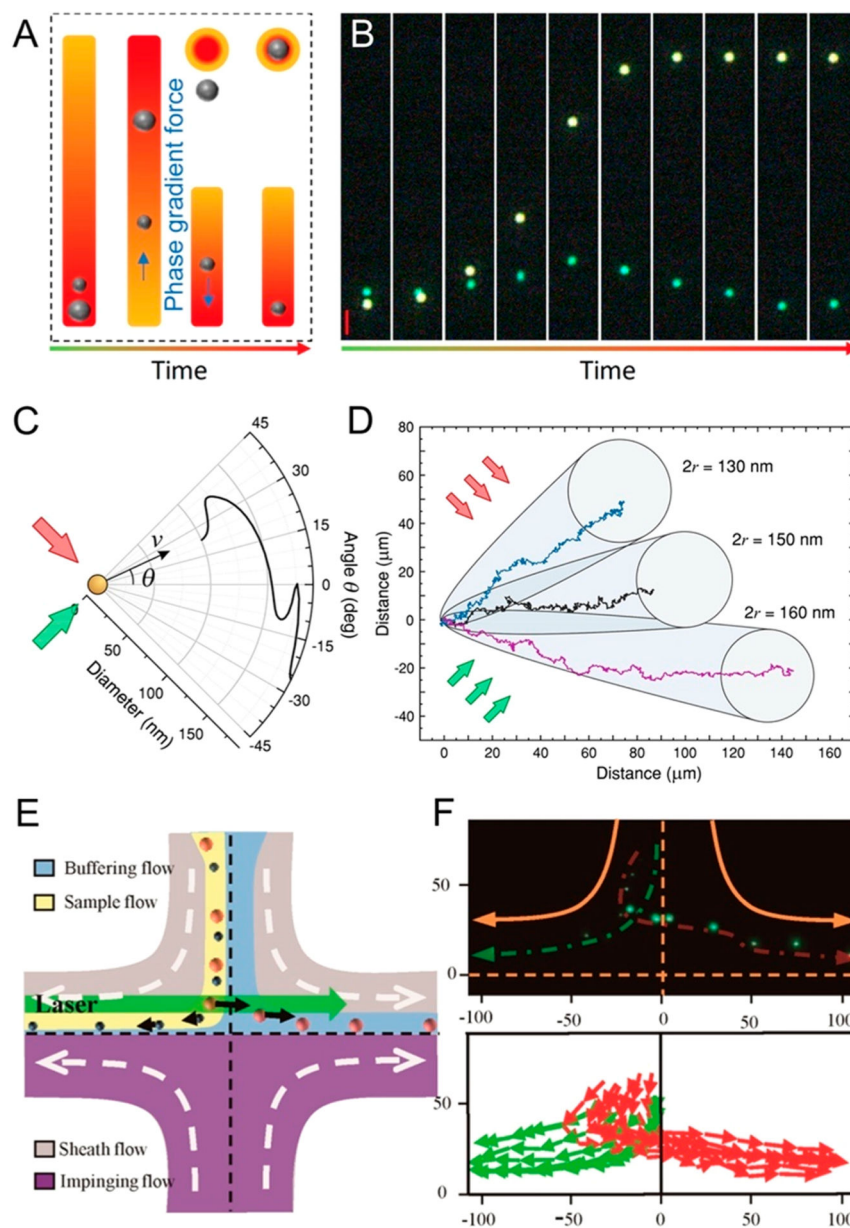


**Figure 10.** Optically enabled nanoparticle separation. (A,B) Nanoparticle separation with phase gradients of light. Reprinted from ref 162. Copyright 2018 American Chemical Society. (C,D) Nanoparticle separation with Mie resonances. Reprinted from ref 163. Copyright 2017 American Chemical Society. (E,F) Nanoparticle separation with a combination of optical and hydrodynamic forces. Reprinted from ref 164. Copyright 2016 American Chemical Society.



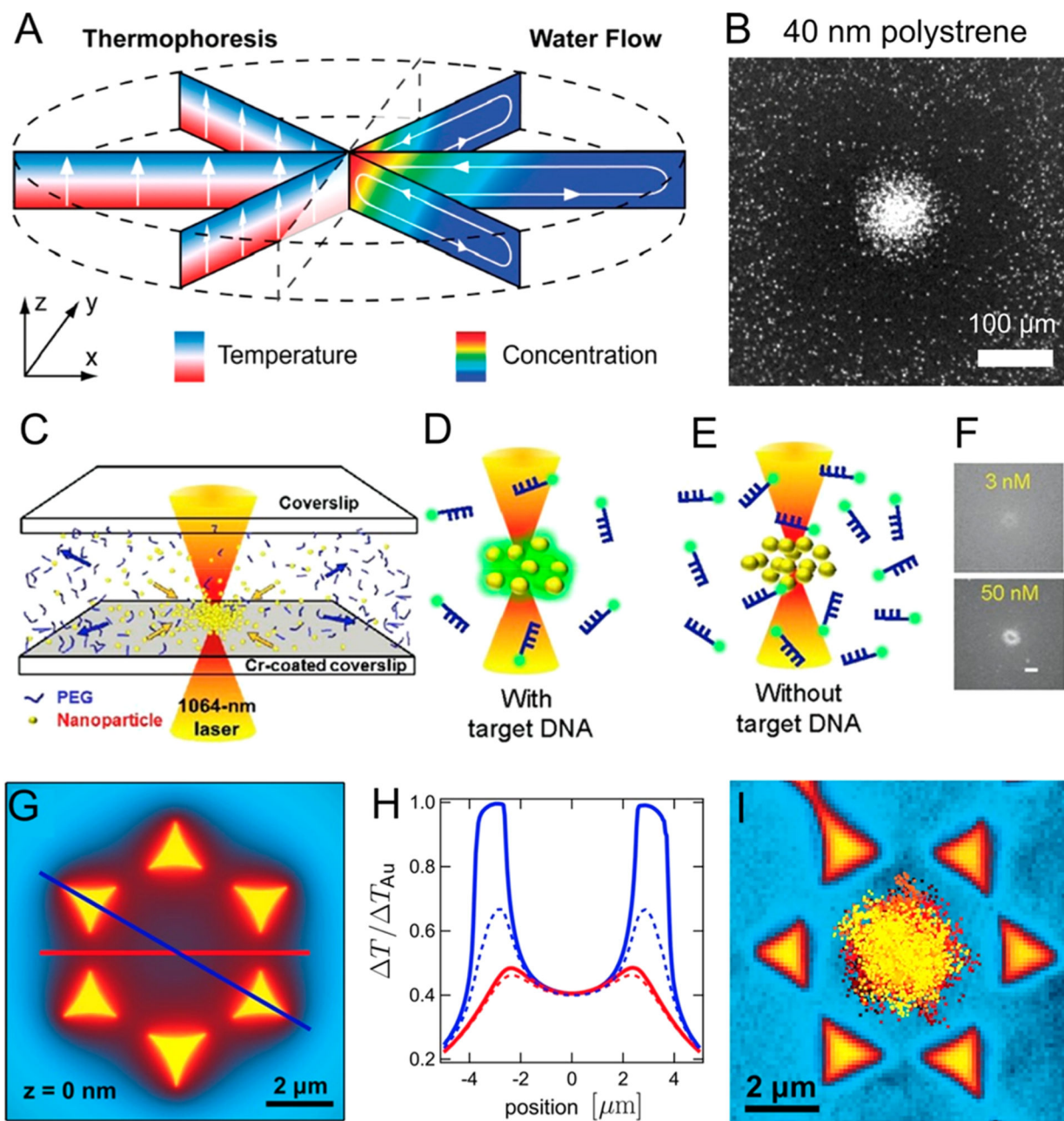


**Figure 11.**

Optical methods to enrich nanoparticles. (A) Mechanism of thermophoretic effect. (B) Its application in concentrating 40 nm polystyrene nanoparticles. Reprinted from ref 170. Copyright 2009 American Chemical Society. (C–F) Using a laser-induced thermophoretic effect to enrich DNA with probes for DNA detection. Reprinted from ref 171. Copyright 2015 American Chemical Society. (G,H) Plasmonic structures regulate the localized temperature distribution. (I) Integrated plasmonic structures utilizing the thermophoretic effect to concentrate nanoparticles at predefined positions. Reprinted from ref 175. Copyright 2013 American Chemical Society.



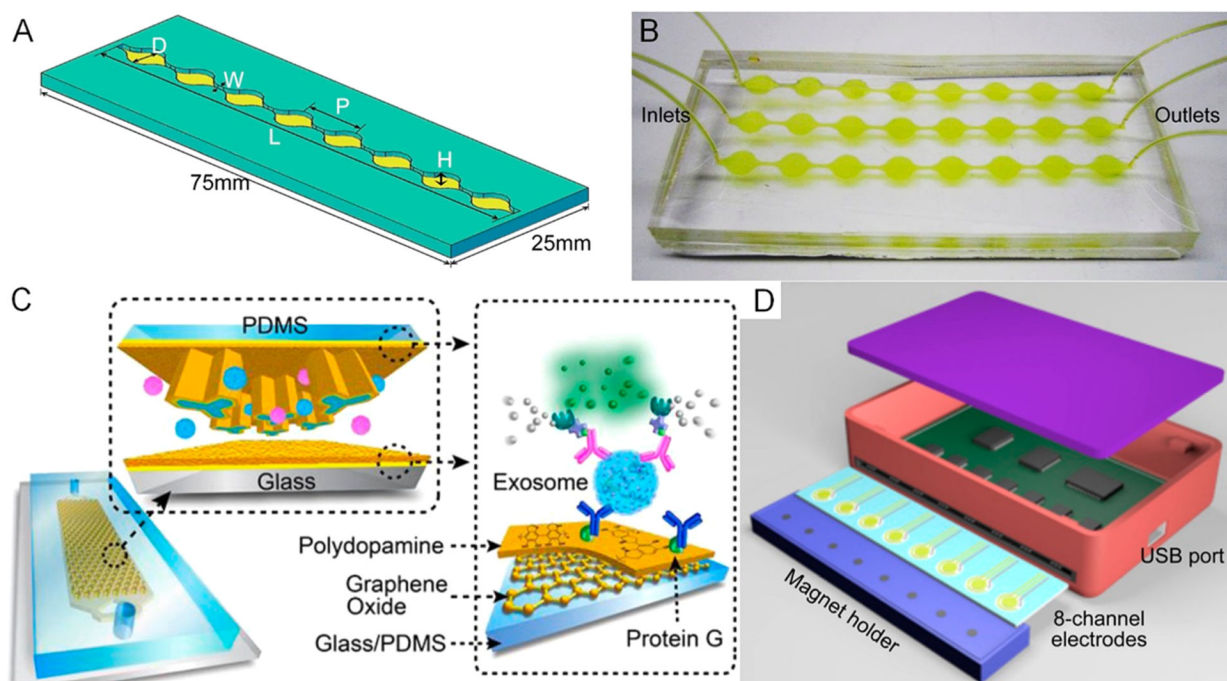


**Figure 12.** Affinity-based nanoparticles isolation. (A) Design of circular shaped microfluidic channels for enhancing exosome capture and (B) a device picture. Reprinted with permission from ref 200. Copyright 2014 Royal Society of Chemistry. (C) Improving exosome capture using a graphene oxide and polydopamine surface coating. Reprinted with permission from ref 202. Copyright 2016 Royal Society of Chemistry. (D) Integrated exosome separation and detection device based on immunomagnetic capture and electrochemical detection. Reprinted from ref 207. Copyright 2016 American Chemical Society.

Table 1.

## List of Particle Isolation Mechanisms Based on Particle Properties

properties	isolation methods	advantages	limitations
size	acoustics	biocompatibility; versatility	force proportional to volume
	dielectrophoresis	valid for most nanoparticles; can also exploit differences in electrical conductivity	force proportional to volume; generate Joule heat; may require special medium
	DLD	do not need external actuation	device clogging
	inertial microfluidics	do not need external actuation	limited size resolution
	microfluidic filtration	do not need external actuation; ease of use	filter clogging; need filter regeneration
	optofluidics	high resolution	low throughput; complex optical setup; low biocompatibility
charge shape	electrophoresis	strong actuation force due to linear scaling law	may require high voltage; generate Joule heat; bubble generation
biochemistry	immunoaffinity separation	high specificity	need labeling procedures; require knowledge of target molecules
polarity	dielectrophoresis	valid for most nanoparticles	mechanism of polarity not entirely clear; generate Joule heat; require special medium